Earth-Science Reviews 113 (2012) 120–140

Contents lists available at SciVerse ScienceDirect

Earth-Science Reviews

journal homepage: www.elsevier.com/locate/earscirev

Late Quaternary hydrological and ecological changes in the hyperarid core of the northern Atacama Desert (~21°S)

Eugenia M. Gayo [a,b], Claudio Latorre [a,b], Teresa E. Jordan [c], Peter L. Nester [c], Sergio A. Estay [a,d], Karla F. Ojeda [b], Calogero M. Santoro [e,f,*]

[a] Departamento de Ecología, Pontificia Universidad Católica de Chile, Casilla 114-D, Santiago, Chile
[b] Institute of Ecology and Biodiversity (IEB), Casilla 653, Santiago, Chile
[c] Department of Earth and Atmospheric Sciences, Cornell University, Ithaca, NY 14853, USA
[d] Instituto de Ciencias Ambientales y Evolutivas, Universidad Austral de Chile. Casilla 567, Valdivia, Chile
[e] Instituto Alta Investigación (IAI), Universidad de Tarapacá, Casilla 6-D, Arica, Chile
[f] Centro de Investigaciones del Hombre en el Desierto (CIHDE). Avda. Gral. Velásquez 1775, Of. 403 Arica, Chile

ARTICLE INFO

Article history:
Received 29 June 2010
Accepted 5 April 2012
Available online 16 April 2012

Keywords:
Dry central Andes
Fossil groundwater
Lowlands
Riparian ecosystems
Tamarugo
Central Andean Pluvial Event

ABSTRACT

The hyperarid core of the Atacama Desert possesses important reserves of "fossil" or ancient groundwater, yet the extent and timing of past hydrologic change during the late Quaternary is largely unknown. *In situ* and/or short-distance transported leaf-litter deposits abound along relict fluvial terraces inserted within four dry and unvegetated valleys that drain into the endorheic basin of Pampa del Tamarugal (PDT, 21°S, 900–1000 m), one of the largest and economically important aquifers in northern Chile. Our exceptional archive offers the opportunity to evaluate the response of low-elevation desert ecological and hydrological systems to late Quaternary climate variability. Three repeated expansions of riparian/wetland ecosystems, and perennial rivers occurred along the southernmost PDT basin between 17.6–14.2 ka, 12.1–11.4 ka and from 1.01–0.71 ka. Both early and late archaic archaeological artefact are present in clear association with our fossil riparian/wetland assemblages, which suggests that these palaeoenvironmental changes facilitated past human occupations in the hyperarid core of the Atacama Desert. Using modern analogues, we estimate that these ecological and hydrological changes were triggered by a threefold increase in rainfall along the headwaters of what are presently inactive canyons. Comparisons with other regional palaeoclimatic records from the central Andes indicate that these changes were synchronous with the widespread pluvial stages now termed the Central Andean Pluvial Event (CAPE— 17.5–14.2 ka and 13.8–9.7 ka). In addition, we summarize new evidence for perennial runoff, riparian ecosystems and a major human settlement during the latest Holocene. Our findings clearly show that local hydrological changes in the PDT were coupled with precipitation variability in the adjacent eastern highlands during the late Quaternary. The long-term dynamics of low-elevation desert ecological and hydrological systems are likely driven by changes in moisture sources, with one source tied to the Amazon region (N–NE mode) and the other to the Gran Chaco region (SE mode). We conclude by linking ENSO-like variability and moisture variations over the Gran Chaco to the three major regional-scale recharge events over the last 18 ka in the PDT basin. We conclude by asserting that an important portion of the groundwater resources in the PDT is indeed fossil, inherited from past pluvial events. We recommend that the relationship between ancient recharge, together with palaeoclimate records of past headwater rainfall fluctuations should be incorporated into future water-balance models and evaluation of groundwater potential in northern Chile.

Contents

Abbreviations: PDT, Pampa del Tamarugal; CAPE, Central Andean Pluvial Event; WAC, Western Andean Cordillera; SM, Sierra de Moreno; AdP Fm, Alto de Pica Formation; SASM, South American Summer Monsoon; QM, Quebrada Maní; QS, Quebrada Sipuca; QT, Quebrada Tambillo; LdS, Lomas de Sal; SI, Similarity Index; SD, standard deviation; SDA, Salar de Atacama; SPN, Salar de Punta Negra; mBGL, meter Below Groundwater Level.

* Corresponding author at: Departamento de Ecología, Pontificia Universidad Católica de Chile, Casilla 114-D, Santiago, Chile. Tel.: +56 2 354 2635; fax: +56 2 354 2621.
E-mail addresses: egayoher@bio.puc.cl (E.M. Gayo), clatorre@bio.puc.cl (C. Latorre).

0012-8252/$ – see front matter © 2012 Elsevier B.V. All rights reserved.
doi:10.1016/j.earscirev.2012.04.003

1. Introduction

By definition, arid regions are always under permanent negative water balance. Yet, these regions also experience major fluctuations in potential evapotranspiration and/or precipitation at different timescales (*e.g.* Lioubimtseva, 2004). The dry central Andes Mountains and adjacent hyperarid Atacama Desert (16°–28°S) have not been an exception. During the late Quaternary, these regions experienced an alternation of arid and wetter conditions (aka pluvial events). Two families of hypotheses have been proposed to explain these patterns. The first is that these resulted as a consequence of low latitude insolation changes over South America and changes in north Atlantic sea surface temperatures (*e.g.* Martin et al., 1997; Baker et al., 2001; Fritz et al., 2004). The second set of hypothesis proposes that pluvial events are driven by insolation changes over the tropical Pacific coupled with atmospheric circulation anomalies along eastern subtropical South America (*e.g.* Latorre et al., 2002; Rech et al., 2002; Quade et al., 2008). According to this hypothesis, the wet (dry) phases in the Atacama Desert are linked to sustained increases (decreases) in summer rainfall forced by enhanced (decreased) tropical Pacific SST gradient and/or increased (decreased) moisture availability in the Gran Chaco basin. Both mechanisms are known major drivers of modern inter-annual and inter-decadal rainfall variability over the central Andes (Vuille et al., 2000; Garreaud et al., 2003; Vuille and Keimig, 2004).

Due to the sensitivity of the central Andes and Atacama Desert to ENSO-like variability, palaeoclimatic reconstructions in these areas have helped elucidate the role of the tropics in driving global climate changes at millennial timescales (Cane and Clement, 1999; Clement and Cane, 1999; Clement et al., 1999; Latorre et al., 2006; Placzek et al., 2006; Quade et al., 2008; Placzek et al., 2009). Furthermore, these reconstructions in concert with palaeoecological studies have provided new insights into the long-term dynamics of local aquifers and lacustrine systems and revealed the extraordinary adaptive capacity of regional ecosystems as well as human societies.

Dramatic changes occurred at 18–9.7 ka in rodent populations and in the latitudinal and altitudinal distributions of plant communities above 2000 m of elevation throughout the western slope of the Andes between 22° and 25°S (Betancourt et al., 2000; Kuch et al., 2002; Latorre et al., 2002, 2003, 2005; Maldonado et al., 2005; Latorre et al., 2006; González, 2008; Quade et al., 2008; Latorre et al., 2009). Palaeohydrological evidence from the central Atacama Desert (22°–24°S) indicates major changes in local water table heights between 15.9 and 9 ka (Betancourt et al., 2000; Bobst et al., 2001; Rech et al., 2002; Lowenstein et al., 2003; Quade et al., 2008). Past lake level fluctuations inferred from abandoned beach terraces indicate several highstands between 18 and 11 ka across the Altiplano (Geyh et al., 1999; Sylvestre et al., 1999; Placzek et al., 2006; 2009). Indeed, such widespread evidence and matching chronologies between these different records have led several authors to postulate that a "Central Andean Pluvial Event" (CAPE) occurred more or less synchronously throughout the region (Latorre et al., 2006; Quade et al., 2008; Placzek et al., 2009).

The impact that these multi-millennial changes in precipitation had on the adjacent lowlands (<2000 m) remains poorly known. Palaeoclimate studies on the timing and impact of past rainfall variability in the lower elevation Atacama Desert are practically non-existent. Examples of questions about potential impacts for which answers are lacking include: did enhanced precipitation at higher altitudes generate a series of flushing events in their aquifers, shifting surface runoff, local water tables and distribution of biota? Is there a relationship between climate change in the lower elevation desert and in the highland central Andes during the late Quaternary? How did past rainfall variability affect the long-term dynamics of these hydrological systems and associated ecosystems? What are the implications of past climate changes for the biogeography of desert communities and modern hydrology?

To answer these questions, we have been studying organic-rich deposits collected along abandoned fluvial terraces inset within hyperarid and plantless canyons that drain into the low-elevation endorheic basin of Pampa del Tamarugal (PDT). In a preliminary report, we presented a palaeoenvironmental and geomorphologic interpretation of fluvial terraces and associated chronology (Nester et al., 2007). Among our major findings were that between 17.4–14.2, ~11.8 and around 1.1–0.7 ka, three repeated expansions of riparian vegetation, associated perennial river-flow and increased local groundwater tables, occurred in the PDT that were synchronous with major pluvial events in the central Andes.

In this paper, we: (1) expand our previous reconstructions on the timing and impact of past climate changes in the northern Atacama Desert with new radiocarbon and macrofossil analyses obtained from 18

new samples of fossil leaf-litter; (2) develop a modern analogue for the PDT fossil assemblages based on present-day plant-communities; (3) use $\delta^{13}C$ measurements on tree-rings from well-dated and taxonomically identified fossil wood to infer past hydrologic change; and (4) discuss the implications of late Quaternary climate changes for the biogeography, hydrology and peopling of the lower elevation Atacama Desert.

2. Regional settings

2.1. Physiographic and geomorphology

The PDT endorheic basin (19°17′–21°30′S) is located in the Central Valley (elevation range 1000–1600 m) within the hyperarid core of the northern Atacama Desert (Fig. 1). The subsurface sedimentary fill of the basin hosts a complex, multi-aquifer groundwater system that spans over 4000 km^2 (JICA, 1995). The basin is bounded by the Coastal Cordillera (a 1000–2000 m altitude range) to the west. To the east, the northern PDT basin (19°17′–21°S) runs up against the foothills of the Western Andean Cordillera (WAC). The southern PDT basin (21°–21°30′S) is flanked to the east by the Sierra de Moreno (SM), a Palaeozoic basement range that rises to 4000 m (Tomlinson et al., 2001) and completely separates the PDT basin from the Altiplano surface drainage basin. Under the modern climate, all of the surface water input to the PDT is from the Andean highlands to the east. Only a few of these eastern streams retain enough surface flow to reach the PDT, and the dominant surface expression of water occurs along the western fringe of the PDT where surface evaporation forces the outcropping of groundwater by capillarity.

The PDT basin dates back to the latest Oligocene–early Miocene with deposition of evaporitic and alluvial/fluvial sediments (Member 1) and volcanic ignimbrites (Member 2) from the Altos de Pica Formation (hereafter AdP Fm). Throughout the Miocene, alluvial sediments (AdP Fm Members 3 and 5) continued to be deposited throughout the

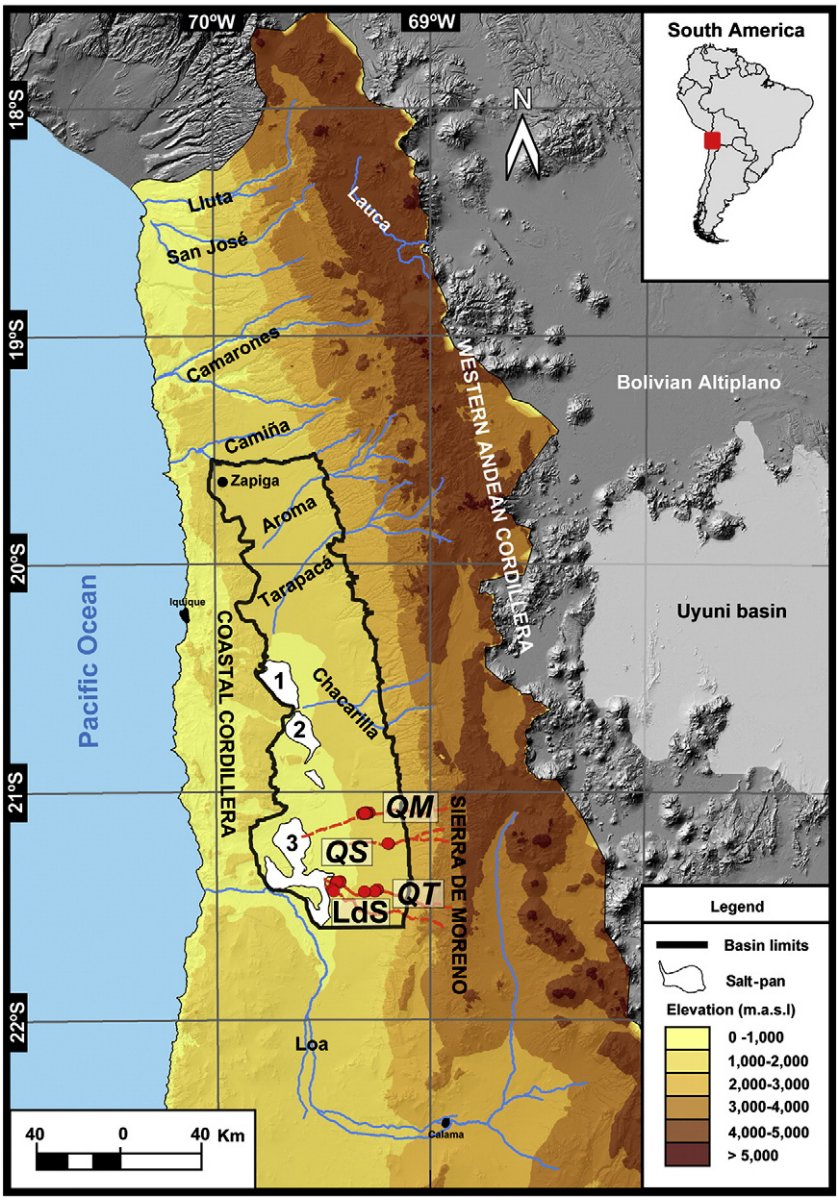

Fig. 1. Study area indicating localities discussed in the text. Locations for the 39 organic-rich deposits analyzed in this study (red circles), unvegetated intermittent canyons from the southernmost PDT basin (orange dashed-lines), perennial streams (blue solid-lines), Salar de Pintados, Salar de Bellavista and Salar de Llamara (numbers 1, 2 and 3 respectively).

basin and ignimbrites (AdP Fm Member 4) accumulated along the eastern flank of the basin. By the latest Miocene–early Pliocene, pediplanation was extensive and a series of deeply incised canyons (>200 m) began to form by groundwater-sapping (Hoke et al., 2004).

A pronounced increase in surface runoff from the SM and WAC during the late Pleistocene led to a series of cut and fill cycles in the southernmost basin (Nester et al., 2007). Thus, late Miocene alluvial fan deposits (T1 in Fig. 2) are inset by a series of late Quaternary abandoned fluvial terraces (T2–T3, Fig. 2) in seven different canyons that drain the SM south of 20°40′S (Fig. 1) (Nester et al., 2007). Terraces are labeled in descending order (to the modern channel) as T1, T2, T2.5, T2.7, T3 and "modern" (Fig. 2). Fluvial aggradational fill associated with terraces T2, T2.5, T2.7, and T3 can reach a thickness of 20 m (Nester et al., 2007). T2 intersects T1 at ~1200 m, spreading beyond this point to form alluvial fans. At Quebrada Tambillo (Fig. 1), the modern channel is inset by 1–3 m at 1250 m elevation and rests >10 m below T3 and continues as a confined channel for several km downstream.

2.2. PDT climate and groundwater

Mean annual temperature (MAT) across the PDT is 19.5 °C, with average minimum and maximum temperatures of −0.2 °C and 33.8 °C during June and December, respectively (Lanino, 2004; DGF, 2007). Evaporation rate values lie in the range of 2000 mm/yr to 3410 mm/yr (DGA, 1987; Lanino, 2004; PRAMAR-DICTUC, 2007) and relative humidity fluctuates between 30% and 59% (JICA, 1995). Mean annual precipitation (MAP) is <1 mm/yr during the last century (DGF, 2007).

Because precipitation is practically nonexistent in the lower desert, the PDT aquifers are recharged by precipitation in catchment basins located in the adjacent eastern highlands, where precipitation increases rapidly with elevation (Houston and Hartley, 2003; Houston, 2006c). Roughly 80% of annual rainfall occurs during the austral summer fed by the South American Summer Monsoon system (SASM; Zhou and Lau, 1998). This seasonal pattern is controlled by the location and strength of the Bolivian High (Garreaud, 1999; Vuille, 1999; Garreaud et al., 2003). Intensification and southward displacement of the Bolivian High enhances the Easterlies flow and increases moisture influx from the Amazon basin and Gran Chaco (Garreaud et al., 2003; Vuille and Keimig, 2004). Inter-annual precipitation variability along the central Andes seems to be controlled by variations in moisture transport linked to: (1) changes in both the intensity/direction of Easterlies winds (modulated by ENSO); and (2) humidity levels over the Gran Chaco (Vuille et al., 2000; Garreaud et al., 2003; Vuille and Keimig, 2004).

Geological and geochemical evidence indicates that two main areas of recharge for PDT aquifers have been inferred to exist along the WAC and SM. The first area is linked to infiltration in the WAC and Altiplano (>4000 m). Magaritz et al. (1990) and Aravena (1995) propose that deep circulation flows through the permeable horizons in the AdP Fm, and this water then outcrops along PDT fault zones. Recharge in the second area takes place via infiltration of surface-water at the apex of alluvial fans at lower elevations (Fritz et al., 1979, 1981; Magaritz et al., 1989, 1990; JICA, 1995; Houston, 2001, 2002, 2006b). This recharge mechanism has been observed to occur on a 4-yr frequency during La Niña events when rare convective storms generate short but intense rainfall at higher elevations (Houston, 2001, 2002, 2006a, 2006b).

The effectiveness of this latter mechanism very likely increases toward the south in the PDT. Houston (2006a) pointed out that mountain-front recharge intensity differs between ephemeral and perennial tributaries. In ephemeral streams, recharge tends to be more intense and effective as the stream is perched above sediments that are not fully saturated with water, which enables rapid infiltration of a large volume of floodwaters. In the case of perennial streams, the shallow sediments adjacent to the stream are saturated with water and flood cannot be infiltrated into the underlying aquifers. Most of the channels that reach the PDT north of ~21°S are perennial, whereas most of those farther south are ephemeral (Fig. 1). This hydrological pattern results from a southward

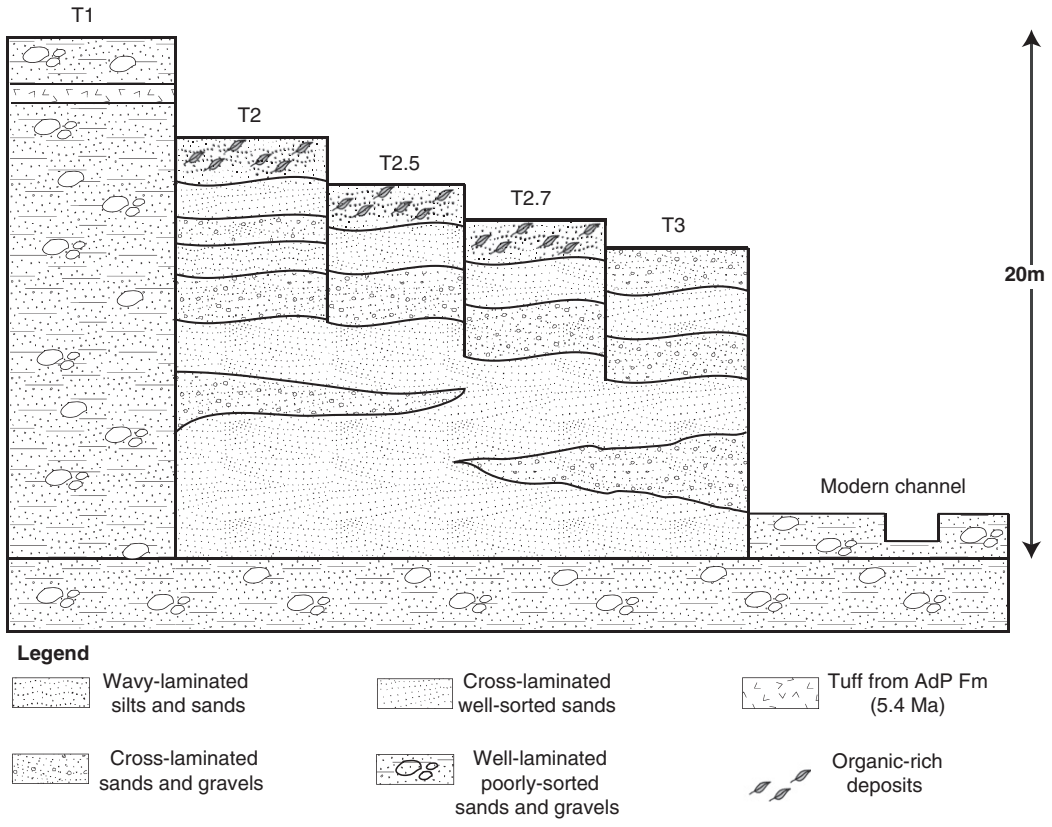

Fig. 2. Generalized stratigraphy of fossil fluvial terraces found along inactive canyons from southern PDT basin (modified from Nester et al., 2007).

decrease in catchment basin area coupled with decreasing mean annual precipitation, which in turn is a function of altitude and latitude (Nester et al., 2007).

2.3. Vegetation

The PDT is dominated by Absolute Desert (Arroyo et al., 1988), a hyperarid landscape of desert pavements that, lacking macroscopic life, are covered by rock fragments in a fine matrix of gypsum and anhydrite (Rech et al., 2003b; Ewing et al., 2006). Nevertheless, both local groundwater discharge and streams create oases for life in this extreme environment.

In the western basin, groundwater discharge feeds natural and reforested Tamarugo communities located along the distal alluvial fan-floodplains and around some salt-pans. These associations are composed mainly of halophytes (*Distichlis spicata*) and phreatophytic taxa such as *Prosopis tamarugo* (Luebert and Pliscoff, 2006). Reforested communities can also incorporate introduced phreatophytes such as *Prosopis alba* and *Prosopis chilensis*.

Riparian ecosystems are common bordering perennial rivers in the northern basin (Gajardo, 1994; Gutierrez et al., 1998; Villagrán et al., 1999). These vegetation formations usually do not extend down into the hyperarid basin, except adjacent the northernmost rivers of Aroma and Tarapacá (Fig. 1). Riparian communities include phreatophytes (*Schinus molle*, *Geoffroea decorticans*), hygrophytes (*Escallonia angustifolia*, *Cortaderia atacamensis*) and halophytes (*Tessaria absinthioides*, *Distichlis spicata*).

In contrast, the riparian vegetation found bordering the ephemeral streams of the southern basin is confined to the spring-fed headwaters. Plants disappear almost completely at altitudes <2300 m. In fact, these areas are essentially barren of vegetation except for the occasional isolated shrub (*Adesmia atacamensis*, *Loasa fruticosa*) and some annuals (*Cistanthe salsoloides*, *Dinemandra ericoides*) growing adjacent to the streambeds after occasional flooding events (Gajardo, 1994).

3. Methods

3.1. Radiocarbon, macro and microfossil analyses

We sampled 39 organic-rich deposits (Appendix A) along four ephemeral tributaries that discharge into the Salar de Llamara in the southernmost PDT basin (21°05′–21°25′S, Fig. 1). Macro and microfossil content analyses and radiocarbon dates from 21 of these deposits were previously reported in Nester et al. (2007) and Gayo et al. (2012) (see Appendix A). Additional two radiocarbon dates on *in situ* roots (N06-11A sample) and $CaCO_3$ rhizoliths (N05-10 sample) were also reported in Nester et al. (2007, see Table 1).

Organic-rich deposits typically occur as mounds (Fig. 3a) preserved on the surface of relict fluvial terraces (T2, T2.5, T2.7, Fig. 2) from Quebradas (canyons) Maní (QM) Sipuca (QS) and Tambillo (QT) (Fig. 3e). We could not locate any of these deposits on the surface of T3. Occasionally, subsurface organic deposits with horizontal stratification are also found in fluvial terraces at depths <30 cm below the surface. In the Lomas de Sal canyon (LdS), organic mounds lie onto the surface of alluvial floodplain deposits (Fig. 3c–d). All mounds and subsurface deposits abound with fossil wood and leaf-litter all of which have no signs of tissue decay and damage (Fig. 3b). Some mounds contain only fossil wood (Fig. 3c), and these were extensively exploited by local "wood hunters" for charcoal production during the nitrate-mining boom (Briones, 1985; Hidalgo, 2009). Practically all the leaf-litter deposits yielded datable and taxonomically identifiable fossil plant remains. Vertically oriented tree trunks often emerge from the mounds and subsurface deposits, suggesting *in situ* past vegetation growth and deposition (Fig. 3c). At LdS, seven of the nine organic deposits described are plant and wood debris accumulated into T2 margins (Fig. 3f, Appendix A).

Between 0.3 and 10 g of plant remains from each organic deposit were submitted for AMS and bulk radiocarbon dates. Short-lived plant tissue (leaves, flowers or twigs) was selected rather than associated logs and bark, except for those organic deposits containing only wood and insufficient fossil leaf remains. Woody plant tissue is particularly resistant to degradation over time in hyperarid environments and many surface wood finds could represent more than one depositional event and thus more than one climate state.

Radiocarbon ages were calibrated using CALIB 6.0 (INTCAL09 calibration curve, Intercept Method). To constrain the significant palaeoclimate events at PDT, we estimated pooled mean ages. All ages reported here are given in thousands of calendar years before 1950 (ka).

Pollen grains from indurated leaf-litter sediments (Appendix A) were extracted using standard techniques (Faegri and Iversen, 1989). Plant macrofossils were separated from leaf-litter deposits under a binocular scope. Microhistological analyses were performed on plant tissues to examine taxonomically relevant characteristics (*e.g.* leaf veins patterns, stomata guard cell shape, trichomes). Microhistological analyses were carried out using a modified protocol based on Latorre et al. (2002). Plant macrofossils were identified to the lowest taxonomic level possible either by comparison with our reference collection of modern flora or by using published taxonomic keys (Muñoz-Pizarro, 1966; Nicora and Rúgolo de Agrasar, 1987). Additionally, fossil trunks with well-preserved cellular details (samples N05-12a, N05-11 and N05-18, Appendix A) were identified from wood anatomical features analyses at the Center for Wood Anatomy Research, USFS Forest Products Laboratory (Madison, WI, US).

3.2. Modern analogue analyses

Five well-defined vegetation formations from the northern Atacama Desert (16°–22°S) serve as potential modern analogues to the fossil plant communities. Among these, the Andean and Altiplano ecosystems encompass species occurring along the WAC semiarid zones at elevations between 2600–3300 m (denoted Andean) and >3400 m (denoted Altiplano) and are watered by direct rainfall. In contrast, the other three associations incorporate species associated with other categories of water sources, such as fog (Lomas formations), groundwater (Pampa formations) and perennial runoff (riparian formations).

We clustered the PDT fossil assemblages into 11 groups based on radiocarbon age, geographical location, stratigraphic position and taphonomy. We also established an additional fossil assemblage for T2.7 at QM, which incorporates two leaf-litter deposits that are awaiting further radiocarbon dating. Taxa not resolved beyond family were excluded from the fossil assemblages.

To identify a modern analogue for the fossil vegetation assemblages, we calculated the similarity between a fossil assemblage and each of the five different modern analogues. The Similarity Index (SI) used was A/B, where A represents the number of species shared between a fossil set and a candidate association, and B is the total number of species within a particular fossil assemblage. The SI ranges from 0 (complete dissimilarity) to 1 (perfect similarity) and was selected to avoid overestimation of similarity due to shared null values. Statistical confidence for each SI was estimated by calculating the standard deviation (SD) from 10,000 bootstraps. All analyses were executed in the R computing environment (R-Development-Core-Team, 2008).

For a given fossil assemblage, the best analogue is the present-day association that possesses the largest SI and smallest SD. When more than one modern association seemed plausible, we used those analogues for which SI is closest to 1 and displayed similar SD. Palaeoenvironmental reconstructions were obtained by directly extrapolating environmental features of the closest analogue to a particular fossil assemblage. If two or more matching analogues were found, mean environmental properties associated with all possible analogues were assigned to the fossil assemblage.

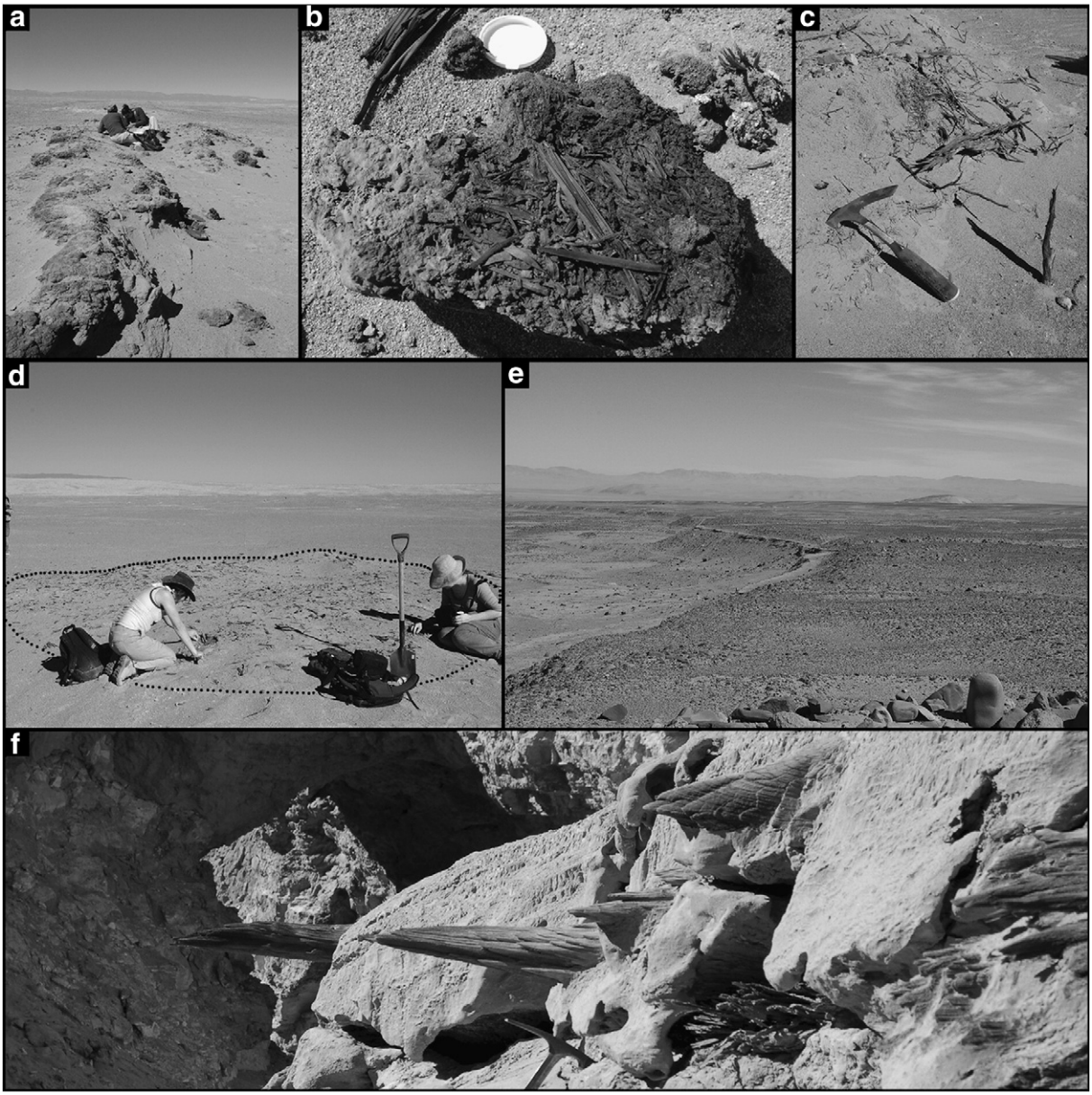

Fig. 3. (a) A fossilized river bank exposed on the T2.5 terrace in the QT valley with (b) fossil plant-remains found in leaf-litter deposits. Note the outstanding preservation of *Cortaderia atacamensis* and *Escallonia angustifolia* leaves, (c–d) *Prosopis tamarugo* mound rising above the surface of alluvial floodplains from the distal segment of LdS. Dotted line in (c) describes a literally "mummified" understory. (e) Panoramic view of hyperarid QM landscape from T2.5 terrace. (f) Flood deposits from LdS containing abundant fossil logs and intercalated horizons of *Escallonia angustifolia* leaves.

Because vegetation distribution in the Atacama Desert is tightly linked to water availability (Arroyo et al., 1988), our palaeoenvironmental reconstructions use the modern precipitation and hydrological conditions associated with the modern analogue assembled to permit qualitative estimates of palaeoprecipitation and palaeohydrological parameters. Present-day MAP ranges for Andean associations were taken from empirical models of the relationship between MAP and altitude along the WAC (Houston and Hartley, 2003). For riparian and Pampa formations, hydrological parameters were taken from governmental or private industry reports (JICA, 1995; DGA, 2004, 2007; PRAMAR-DICTUC, 2007), available literature (Rojas and Dassargues, 2007) and open-access information available at the Dirección General de Aguas website (http://www.dga.cl). Environmental parameters associated with the modern Lomas formations are from Cereceda et al. (2008).

3.3. Stable isotope analysis

Carbon isotopes of annual tree rings were analyzed in a ^{14}C-dated cross-section of *Schinus molle* fossil wood from the LdS flood deposits (sample N05-12A, Appendix A). Identification of annual tree-rings and width measurements were carried out under a binocular scope using a ruler with a precision of 0.5 mm.

Ten mg of latewood and earlywood fractions was extracted at regular intervals of two tree-rings using a rotary drill with a 1 mm diameter drill bit. Additionally, we sampled five consecutive tree-rings by employing the same procedure. Isotope analyses are on both whole-wood tissue (untreated) and crude cellulose (treated). Crude cellulose extraction process followed the Diglyme-HCl method of MacFarlane et al. (1999). Cellulose extractions on five tree-rings were conducted to assess potential effects of either mobile components or non-climatic

process on $\delta^{13}C$ values from untreated whole-wood tissue. Comparisons among $\delta^{13}C$ values for untreated and treated samples were evaluated using Pearson correlations.

The $\delta^{13}C$ of treated and untreated tree-ring materials was measured at the Cornell University Stable Isotope Laboratory (COIL, Ithaca, NY, US). Results are reported in δ notation in permil (‰) deviations from the V-PDB standard. Precision for these analyses was ± 0.1‰.

4. Results

4.1. Stratigraphy and radiocarbon chronology

Leaf-litter deposits occur in four different stratigraphic contexts. The most common types of these deposits are leaf-litter and wood mounds that rise slightly above the average surface elevation of the fluvial terraces that form benches on canyon walls. These organic-rich deposits are contained within fine sandy silts and represent fossilized understories of vegetation growing *in situ* upon the terrace surface (Fig. 3a). Thus, ^{14}C-dates on plant remains from the mounds provide a minimum age estimate for the end of a particular aggradational sedimentation event.

A second type of deposit is leaf-litter mounds that emerge onto the surface of alluvial floodplains located along the distal segment of LdS (Fig. 3c–d). These are contained in fine silts and likely correspond to *in situ* vegetation growing in areas that experienced occasional flood events originated as runoff from the adjacent highlands.

In situ subsurface leaf-litter deposits can also occur beneath terrace surfaces. This third type of deposit appears as dispersed or concentrated plant material embedded within a wavy-laminated fine silt or sand matrix (Fig. 4a), likely indicating an overbank depositional environment. Therefore, these represent *in situ* vegetation that grew in areas with periodic flooding and/or ponding. Vertical successions of horizontal layers reflect historical series of sediment aggradation and stream events as well as changes in the depositional environments. For example, a thin bed of well-sorted fine to medium cross-bedded sands underlying all subsurface leaf-litters (Fig. 4a) could indicate in-channel or floodplain sandbar deposits. In contrast, deposition of a thin layer of desert pavement at the top of T2.5 and T2.7 from QT could imply a switch from fluvial to aeolian deposition. Similarly, a thin layer of horizontal bedded fine to medium-grained sands (Fig. 4a) above the QM-2E deposit suggests that it was buried completely by aeolian deposition between 0.81 and 0.78 ka, as indicated by the presence of *in situ* fossil canes.

Finally, the fourth type of deposit incorporates plant and wood debris contained in fine-grain silty layers at LdS (Fig. 4b). These deposits likely reflect some degree of transport drifted onto the T2 margins as flood loads (Figs. 3f, 4b) and were later covered by colluvial sediments at LdS-1 (Fig. 3f). These log-jam deposits (aka flood deposits) include leaves, seeds, twigs and inflorescences as well as large to medium logs typically imbricated or horizontally-oriented with respect to the riverbed (Figs. 3f, 4b).

Based on 30 radiocarbon dates of *in situ* and log-jam deposits we provide a record of ecological and hydrological changes in the lower elevation Atacama Desert spanning the last 18 ka (Table 1). Our ^{14}C-chronology shows definite clustering at ~13.5 and at ~0.87 ka. Two distinct hiatuses are evident in our deposits between ~13.9 and 12.3 ka and practically for the entire Holocene (Table 1, Fig. 5).

Two sub-clusters of dates occur within the latest Pleistocene (Fig. 5). The first group (n = 17 dates), clustering at 15.4 ka, includes dates from rootlets preserved in $CaCO_3$ rhizoliths within T2 terrace at QS and *in situ* leaf-litter (mounds and subsurface deposits) preserved upon T2 (17.6–15.6 ka), T2.5 (15.9–15.7 ka) and T2.7 (15.8–15.3 ka, Table 1). Clusters also occur for *in situ* (15.3–14.6 ka) and flood deposits (15.0–14.2 ka) from the LdS (Table 1, Fig. 5). The second group (n = 7 dates) of latest Pleistocene dates (11.8 ka, Fig. 5) incorporates plant-remains from LdS-6 flood deposits (12.1–11.8 ka), *in situ* roots found within fan deposits at the distal portion of LdS (N06-11 A sample, Table 1) and *in situ* grass-stems (12.0–11.4 ka) found on the surface of T2.5 at QM (Table 1, Fig. 5).

A latest Holocene cluster (~0.87 ka, Fig. 5) includes six radiocarbon dates on plant remains from *in situ* leaf-litter deposits collected on the surface of T2.5 within QM (Table 1, Fig. 5).

4.2. Micro and macrofossil analyses

We analyzed 37 organic-rich deposits for plant macrofossils. Further two samples of indurated sediments were analyzed for pollen (Appendix A). The macrofossil array of these deposits includes well-preserved feathers, rodent and avian faeces, insects, leaves, seeds, fruits, twigs and inflorescences. We identified macrofossils from 28 taxa in 13

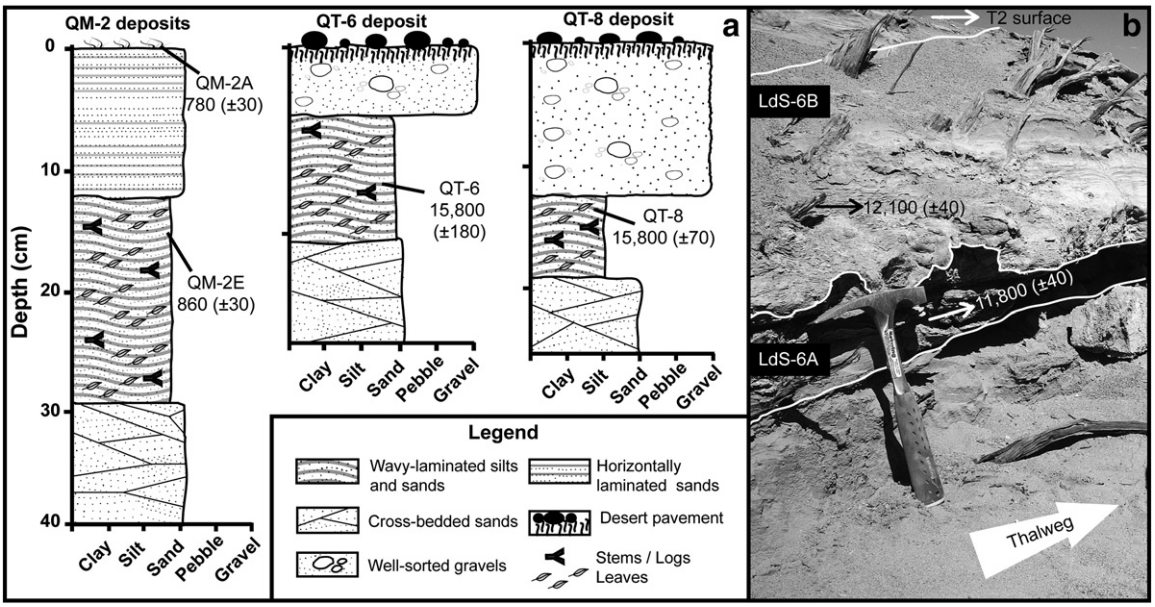

Fig. 4. (a) Stratigraphic sections for subsurface deposits of situ leaf-litters at QM (section QM-2) and QT (sections QT-6, QT-8). Dated samples QM-2A and QM-2E recovered from T2.5 terrace are also shown. QT-6 was described from T2.7, whereas QT-8 is part of the T2.5 terrace. (b) A log-jam flood deposit embedded along the T2 terrace wall at LdS-6. Note the imbricated logs at LdS-6A. All radiocarbon dates are in calendar years BP (see Table 1).

Table 1
Radiocarbon dates for organic-rich deposits from southern PDT basin.

No.	Sample ID	Laboratory code	Dated material	^{14}C yr BP	δ^{13}C (‰)	Calibrated age (ka BP)	2σ (cal. yr BP)
Quebrada Maní (QM)							
1	QM-2A[a,b]	CAMS-129007	Canes	870 ± 30	−10.4	0.78	−45/115
2	QM-2E[a,b]	CAMS-129008	Twigs	960 ± 30	−22.7	0.86	−55/70
3	QM-3[a,b]	CAMS-129009	Leaves	1110 ± 30	−24.3	1.01	−35/45
4	QM-4[b,c]	CAMS-131272	Leaves	13,190 ± 35	−24.3	15.6	−180/150
5	QM-14[a,d]	UGAMS-4065	Twigs	790 ± 25	−22.9	0.71	−20/15
6	QM-15A[a]	UGAMS-4066	Stems	10,260 ± 40	−25.5	12.0	−180/70
7	QM-15B[a]	UGAMS-4561	Stems	10,110 ± 30	−24.7	11.7	−110/90
8	QM-16[a,d]	UGAMS-4067	Leaves	810 ± 25	−26.2	0.72	−20/20
9	QM-17[a]	UGAMS-4562	Stems	10,030 ± 40	−25.6	11.5	−130/90
10	QM-18[a,d]	UGAMS-4563	Leaves	990 ± 25	−21.7	0.92	−115/15
11	QM-19[a]	UGAMS-4564	Stems	9960 ± 40	−22.5	11.4	−120/210
Quebrada Sipuca (QS)							
12	QS-1[b,c]	GX-32394	Leaves	13,330 ± 80	−24.3	15.8	−220/190
13	QS-3[a,b]	GX-32395	Leaves	13,400 ± 70	−24.4	15.9	−210/180
14	N05-10[b]	UCIAMS-29222	*In situ* rhizoliths within T2	14,470 ± 70	No data	17.6	−140/225
Quebrada Tambillo (QT)							
15	QT-1[b,c]	GX-32396	Leaves	13,290 ± 80	−23.9	15.8	−210/190
16	QT-5[b,e]	GX-32397	Leaves	12,940 ± 150	−24.8	15.3	−242/210
17	QT-6[a,b]	GX-32398	Leaves	13,310 ± 180	−24.5	15.8	−320/280
18	QT-8[b,e]	CAMS-129367	Leaves	13,280 ± 70	−24.0	15.8	−210/180
19	QT-9[a,b]	CAMS-131273	Leaves	13,220 ± 35	−27.1	15.7	−180/160
20	N05-11[a,b]	UCIAMS-292220	Wood	13,080 ± 30	−20.5	15.9	−320/390
Lomas de Sal (LdS)							
21	LdS-1[f]	UCIAMS-29216	Leaves	12,400 ± 192	No data	14.5	−360/310
22	LdS-5[g]	UGAMS-4559	Leaves	12,630 ± 40	−22.2	14.9	−130/120
23	LdS-6A[f]	UGAMS-4062	Twigs	10,120 ± 40	−22.2	11.8	−140/360
24	LdS-6B[f]	UGAMS-4063	Twigs	10,320 ± 40	−21.4	12.1	−90/210
25	LdS-7[g]	UGAMS-4560	Bark	12,950 ± 40	−24.8	15.3	−140/120
26	LdS-8[g]	UGAMS-4064	Flowers	12,490 ± 40	−27.2	14.6	−190/200
27	N04-14A[b,f]	AA-62290	Leaves	12,244 ± 96	−28.1	14.2	−190/130
28	N05-12A[b,f]	UCIAMS-29218	Wood	12,735 ± 30	−20.2	15.0	−100/90
29	N05-18[b,f]	UCIAMS-29219	Wood	12,435 ± 30	−20.7	14.5	−200/130
30	N06-11A[b]	UCIAMS-29219	*In situ* roots within fan deposits	10,170 ± 70	−21.7	11.8	−132/155

[a] Mound or subsurface *in situ* deposits onto T2.5 terrace.
[b] Reported previously in Nester et al. (2007).
[c] Mound or subsurface *in situ* deposits onto T2 terrace.
[d] Reported previously in Gayo et al. (2012).
[e] Mound or subsurface *in situ* deposits onto T2.7 terrace.
[f] LdS log-jam deposits.
[g] *In situ* mounds found onto alluvial floodplains from LdS.

families (Table 2, Appendix A). The number of taxa per organic-rich deposit ranges from a minimum of one to a maximum of 14 (Appendix A).

All *in situ* leaf-litter deposits from fluvial terraces at QM, QS and QT dated at 15.9–14.2 ka, (Table 1) are broadly dominated by taxa presently absent from this area such *Schinus molle* and *Escallonia angustifolia* remains (Fig. 6a–b, Appendix A). At QS and QT *Tessaria absinthioides*, *Baccharis scandens*, *Cistanthe* sp and *Cortaderia atacamensis* macrofossils were also present on the T2.5 and T2.7 terraces (Fig. 6c–e, Appendix A). Pollen analyses on two *in situ* indurated leaf-litter deposits collected at QS and QT canyons reveal that Asteraceae sp, Poaceae sp and *Prosopis tamarugo* have occurred on the surface of T2 terrace (Appendix A). Most *in situ* organic-deposits from the alluvial flood plain LdS that dated to 15.3–14.6 ka (Table 1, Appendix A) array *Distichlis spicata*, *Tessaria absinthioides* and abundant macrofossils of *Prosopis tamarugo* (Fig. 6f–

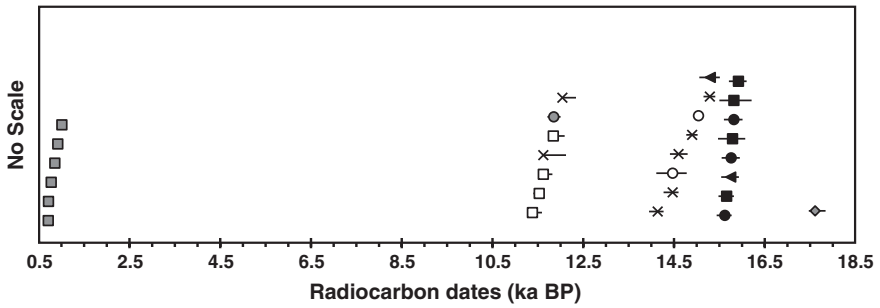

Fig. 5. The distribution of 30 radiocarbon dates (in ka) on plant-remains from the southernmost PDT basin. (gray diamond) Rootlets preserved in rhizoliths at T2 within QS canyon, (dark circles) *in situ* leaf-litter deposits collected along the T2 terrace, (dark squares) *in situ* leaf-litter deposits on T2.5, (dark triangles) *in situ* leaf-litter deposits onto T2.7, (gray circle) *in situ* roots in alluvial fan deposits from the western portion of LdS canyon, (x) *in situ* deposits found at LdS, (open circles) flood deposits from LdS, (open squares) *in situ* grass-stems deposits from QM, (gray squares) *in situ* deposits from QM canyon.

Table 2
List of plant taxa identified from macro and microfossil analyses. Functional group for each species was defined based on both phenology and water-use strategies: (Pe) perennial, (An) annual, (H) halophyte, (Hy) hygrophyte, (X) xerophyte, (Ph) phreatophyte, (Cu) cultivated. Taxa distribution at major Northern Atacama Desert vegetational formations: (R) riparian, (L) Lomas, (P) Pampa, (A) Andean, (AL) Altiplano, (extra-local) currently not present.

No.	Taxon	Family	Functional group	Material indentified	Distribution
1	*Asteraceae* sp	Asteraceae	No data	No data	No data
2	*Atriplex atacamensis*	Chenopodiaceae	Pe, H	Leaves, stems, fruits and panicles	R, P, A, AL
3	*Atriplex glaucescens*	Chenopodiaceae	Pe, H	Fruits and leaves	R, A, AL
4	*Atriplex imbricata*	Chenopodiaceae	Pe, H	Leaves, stems and fruits	R, P, A, AL
5	*Atriplex* sp	Chenopodiaceae	Pe, Hy	Fruits	No data
6	*Baccharis alnifolia*	Asteraceae	Pe, Hy	Achenes	R
7	*Baccharis scandens*	Asteraceae	Pe, Hy, H	Flowers, achenes and leaves	R
8	*Chenopodium petiolare*	Chenopodiaceae	An, Hy, X	Seed	R, L, A, AL
9	*Cistanthe* sp	Portulacaceae	An, Hy, X	Leaves, stems, seeds and flowers	R, L, A, AL
10	*Caesalpinia aphylla*	Caesalpiniaceae	Pe, Ph	Flowers	P
11	*Cortaderia atacamensis*	Poaceae	Pe, Hy	Anthecium and blades	R, A, AL
12	*Cryptantha* sp	Boraginaceae	An, Hy, X	Leaves and stems	R, A, AL
13	*Distichlis spicata*	Poaceae	An, H	Stems	R, P, A, AL
14	*Escallonia angustifolia*	Escalloniaceae	Pe, Hy	Leaves and flowers	R
15	*Euphorbia amandi*	Euphorbiaceae	An, X	Seed and fruit	AL
16	*Junellia* sp	Verbenaceae	Pe, X	Seeds	A, AL
17	*Muhlenbergia* sp	Poaceae	An, Hy	Anthecium	R, A, AL
18	*Nicotiana longibracteata*	Solanaceae	Pe, Hy	Seed	R
19	*Poaceae* sp	Poaceae	No data	Pollen grain	No data
20	*Polypogon interruptus*	Poaceae	Pe, Hy	Flower sterile husk	R, AL
21	*Prosopis tamarugo*	Mimosaceae	Pe, Ph	Leaves, twigs, wood, bark, flowers, pods, seeds	R, P
22	*Schinus molle*	Anacardiaceae	Pe, Ph	Wood, flower, fruits	R
23	*Stipeae* sp	Poaceae	No data	Stems	A, AL
24	*Solanaceae* sp	Solanaceae	No data	Seed	No data
25	*Solanaceae* sp2	Solanaceae	No data	Seed	No data
26	*Tarasa operculata*	Malvaceae	Pe, Hy, X	Seed	R, A, AL
27	*Tessaria absinthioides*	Asteraceae	Pe, H	Achenes	R, L, P
28	*Zea mays*	Poaceae	An, Cu	Canes	Extra-local

h). Exceptionally, at the alluvial flood plain of LdS an *in situ* leaf-litter deposit (LdS-5 sample) dated in 14.9 ka arrays *Caesalpinia aphylla*, *Escallonia angustifolia*, *Tessaria absinthioides* and *Schinus molle* remains (Table 1, Appendix A).

Cuticle analyses on *in situ* stems preserved onto T2.5 at QM (12.0–11.4 ka, Table 1) argue for the presence of a grass with epidermal features that did not exhibit any similarities with the current gramineas found today in the northern Atacama. Actually, these analyses on these fossil grasses revealed elongated epidermal cells with fine-narrow undulating margins (Fig. 6h), a diagnostic character for the Stipae tribe (Poaceae; Matthei, 1965) (Fig. 6i, Appendix A).

Macrofossil analysis of organic-flood sediments from the LdS canyon dated at 14.5–14.2 ka reveals similar assemblages to those present within *in situ* leaf-litter deposits occurring onto the fluvial terraces at QM, QS and QT between 15.9 and 14.2 ka (Table 1, Appendix A). Younger plant debris deposits from LdS (12.1–11.8 ka, Table 1) are considerably less diverse and contain abundant twigs and leaves of *Prosopis tamarugo* leaves along with *Cistanthe* sp seeds (Appendix A).

The youngest *in situ* leaf-litter deposits from the latest Holocene are much richer, including nearly 13 new taxa such as *Baccharis alnifolia*, *Atriplex atacamensis*, *Euphorbia amandi*, *Chenopodium petiolare*, *Polypogon interruptus*, and *Cryptantha* sp, among others (Fig. 7, Appendix A). Most of these deposits contained considerable amounts of *Prosopis tamarugo* macrofossils as well as taxa recorded in the latest Pleistocene deposits (*e.g. Cortaderia atacamensis*, *Baccharis scandens*, *Tessaria absinthioides* and *Cistanthe* sp). Interestingly, cultivated corn (*Zea mays*) was also present in these deposits.

Undated *in situ* leaf-litters collected from the T2.7 at QM (samples QM-8 and QM-9, Appendix A) incorporate taxa recorded in latest Pleistocene and latest Holocene deposits (*Tessaria absinthioides*, *Cistanthe* sp and *Prosopis tamarugo*).

4.3. Modern analogue analyses

Practically all leaf-litter deposits preserved on the fluvial terraces (Table 3, assemblages 1–6) and flood deposits from LdS (assemblages 8–9) match present-day riparian formations. This implies that perennial river flow and higher water table elevations existed within the southern PDT basin during the interval 15.9–14.2 ka and again at 12.1–11.8 ka. By extrapolating modern hydrological parameters from eight perennial rivers (Table 4), late Glacial–early Holocene perennial streams might be related to mean annual discharge that ranged from 2.07 to 0.16 m^3/s.

Today, the water table at LdS reaches a depth of ~70 mBGL (PRAMAR-DICTUC, 2007), whereas present-day Pampa vegetation formations are restricted to locations where phreatic levels range from 0 to 25 mBGL (JICA, 1995; PRAMAR-DICTUC, 2007; Rojas and Dassargues, 2007). The plant debris in the LdS *in situ* deposit (Table 3, assemblage 7) closely resembles the modern Pampa formation. Hence, this association suggests that the phreatic levels were locally ~45 m higher from 15.3 to 14.6 ka than today.

A latest Holocene leaf-litter deposit on T2.5 at QM (Table 3, assemblage 10) bears important similarities with riparian, Andean and Altiplano formations, suggestive that the corresponding past precipitation (>67 mm/yr, Houston and Hartley, 2003) was higher than today and past perennial runoff was 2.8 and 0.22 m^3/s (DGA, 2004) in QM. On the contrary, equivalent SI scores among candidates and large overlapping SD (Table 3) indicate that assemblage 11 lacks modern analogues. Palaeoenvironmental reconstruction on the T2.7-QM assemblage suggests concurrently perennial river flows, increased elevation of the local water table under hyperarid conditions, relative humidity >70% by strong fog influence (Cereceda et al., 2008) and increased local precipitation (>67 mm/yr, Houston and Hartley, 2003).

4.4. $\delta^{13}C$ in tree-rings

We obtained a $\delta^{13}C$ record from 45 tree rings of a *Schinus molle* fossil log dated at 15 ka (N05-12A sample, Table 1). $\delta^{13}C$ values in whole-wood tissue and cellulose of −22.2 to −20.4‰ (Fig. 8) are within the range of those described for C_3 plants. Whole-wood tissue $\delta^{13}C$ from tree-rings was not significantly different than crude cellulose, exhibiting a fairly good correlation (Pearson $r = 0.87$, $p < 0.1$) and both exhibit an almost identical trend (Fig. 8).

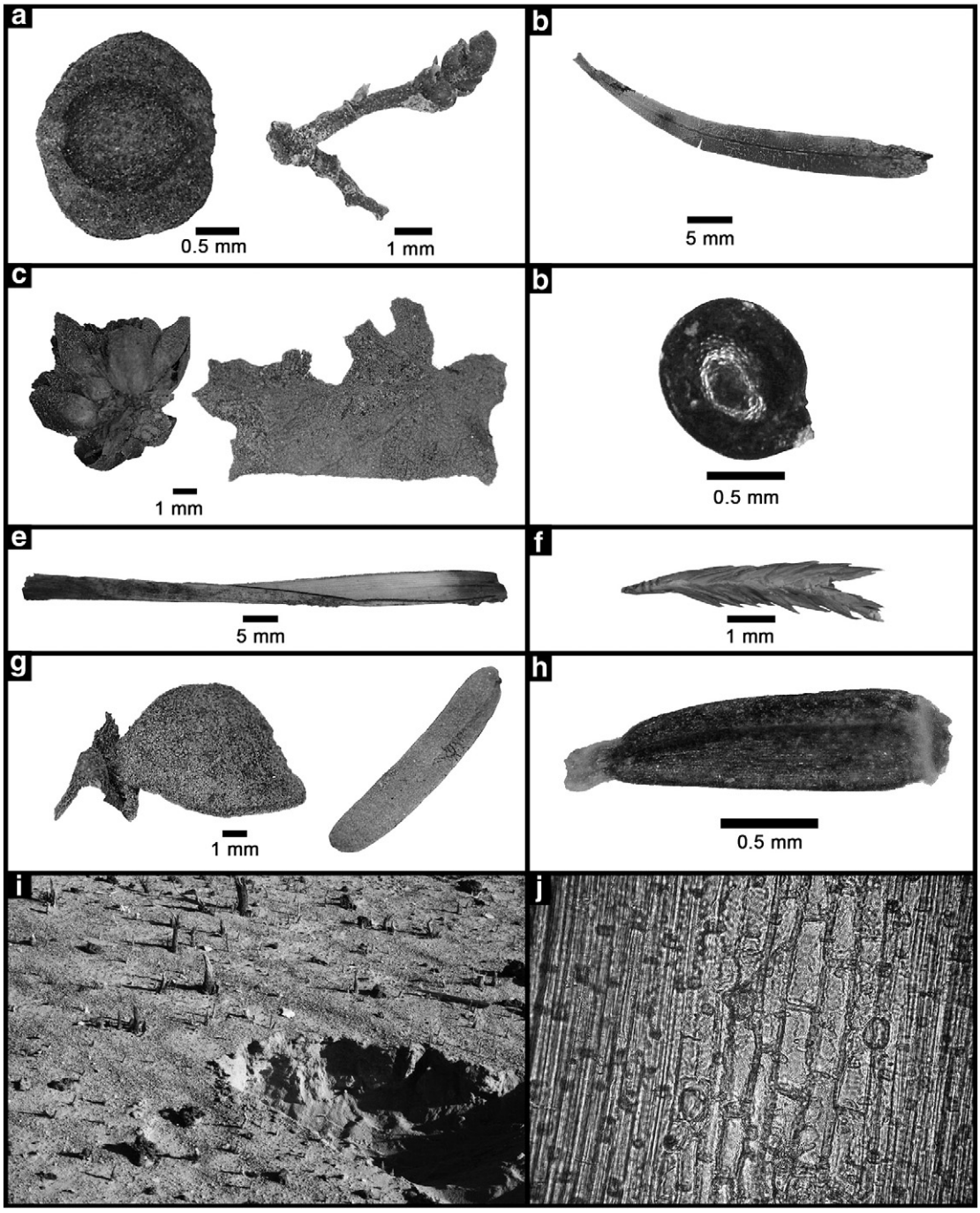

Fig. 6. Photographs of plant-macrofossils from latest Pleistocene leaf-litter deposits. (a) *Schinus molle* fruit and inflorescence, (b) *Escallonia angustifolia* leaf, (c) *Baccharis scandens* flower and leaf, (d) *Cistanthe* sp seed, (e) *Cortaderia atacamensis* blade, (f) *Distichlis spicata* stem, (g) *Caesalpinia aphylla* flower and *Prosopis tamarugo* leaf, (h) *Tessaria absinthioides* achene, (i) *in situ* Stipeae sp stems at QM, (j) Details of Stipeae cuticle features (at 40×).

Carbon isotope ratios between tree rings 2 and 6 exhibit negative values with a steady mean of −21.9‰ (Fig. 8). An abrupt shift toward more positive values (from −20.7 to −21.9‰) occurs between rings 6 and 10. These positive values (mean = −20.5‰) persist from tree-rings 12 to 16 (Fig. 8). Pronounced variations in $\delta^{13}C$ occur between rings 18 and 30 (mean = −21‰). Marked variations in $\delta^{13}C$ values remain between rings 32 and 62, however, $\delta^{13}C$ values are more negative (mean = −21.9‰). Ring-to-ring oscillations are evident between the rings 58 and 62 (Fig. 8). Tree-rings 62–68 indicate a rapid increase in $\delta^{13}C$ values which again decrease between rings 68 and 72. The overall trend becomes significantly more positive (average −21.2‰) from ring 72 to 80 after which they drop quickly to −21.7‰ at ring 86.

5. Discussion

5.1. Palaeoecology of the southern PDT basin

The low taxonomic richness (from 1 to 14 taxa, Appendix A) apparent at each organic deposit is likely related to taphonomy. As previously noted in Section 4.1, *in situ* trunks and leaf-litters in mounds and subsurface deposits represent fossilized understories. The extensive mounds of *Prosopis tamarugo* preserved on the surface of alluvial floodplains at LdS (Fig. 3d) are clearly a projection of the area of individual canopies that in modern forests occupy an area of ~145 m^2 per tree (Covarrubias et al., 1994). Thus, these deposits are discrete

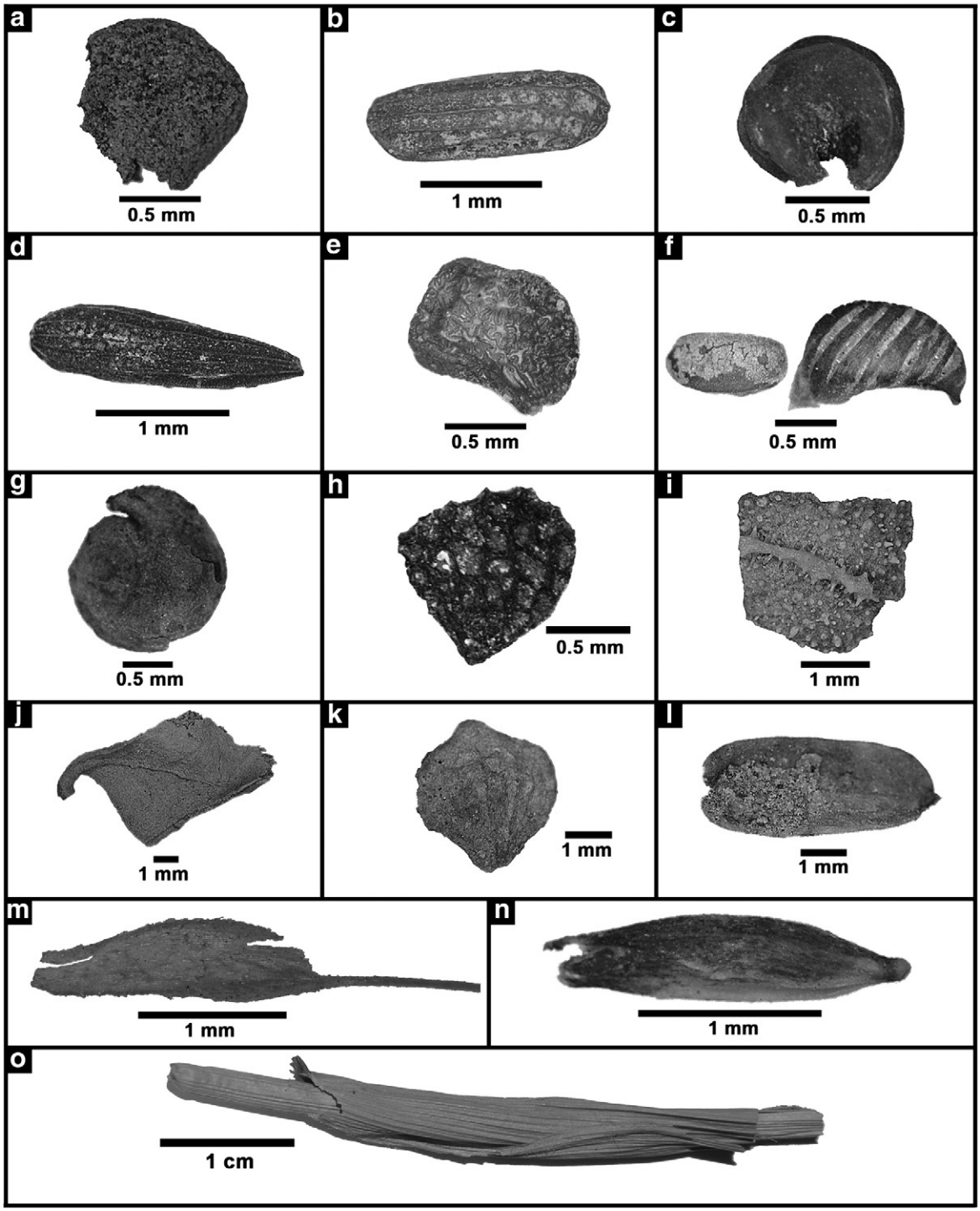

Fig. 7. Photographs of plant-macrofossils from latest Holocene leaf-litter deposits. (a) *Chenopodium petiolare* seed, (b) *Junellia* sp seed, (c) *Tarasa operculata* seed, (d) *Baccharis alnifolia* achene, (e) *Nicotiana longibracteata* seed, (f) *Euphorbia amandi* seed and fruit, (g) Solanaceae seed 1, (h) Solanaceae incomplete seed 2, (i) *Cryptantha* sp leaf, (j) *Atriplex atacamensis* leaf, (k) *Atriplex* sp fruit, (l) *Atriplex glaucescens* leaf (m), *Polypogon interruptus* floret, (n) *Muhlenbergia* sp floret, (o) *Zea mays* culm and ligule.

records of past vegetation growth, preserving limited areas of a particular terrace that eventually incorporated remains from neighbouring plants and animals that directly foraged underneath the canopy. In contrast, log-jam deposits are accumulations of broken plant organs or entire individuals that lived near the riverbed. Therefore, these deposits provide a biased view of the riparian vegetation occurring upstream and that was subsequently uprooted and transported downstream as part of a flood load. Overall, the PDT fossil record shows important palaeoecological changes in the lower-elevation desert during the late Quaternary. In fact, our results indicate that during the last 18 ka at least three distinct expansions of riparian/wetland formations occurred in the southernmost PDT basin (Fig. 5).

In the interval 15.9–14.2 ka, riparian communities expanded into what are now plantless canyons. These palaeocommunities, represented by assemblages 1–6 and 8 (Table 3), exhibit similar taxonomical composition and blend of functional groups (hygrophyte, phreatophyte and halophyte, Table 2) to ecosystems confined today to perennial streams found north of 21°S (Gajardo, 1994). An additional ^{14}C date on rootlets preserved in $CaCO_3$ rhizoliths within the sedimentary sequence of the T2 terrace (Nester et al., 2007) extends the presence of riverside

Table 3
Similarity matrix. Standard deviations are in brackets. ID first term refers to stratigraphic position and/or depositional feature. T2, T2.5, T2.7: correspond to *in situ* deposits collected at the terrace sequences defined by Nester et al. (2007, see Fig. 2). Flood: organic-rich deposits found within flood sediments drifted onto T2 margins at LdS. Floodplain: refers to *in situ* deposits located along the distal segment of LdS. Second term indicates origin (see Section 3.1 for further explanation of abbreviations).

No.	Fossil assemblage ID	Riparian formation	Lomas formation	Pampa formation	Andean formation	Altiplano formation
1	T2-QM	1 (0)	0 (0)	0 (0)	0 (0)	0 (0)
2	T2-QS	1 (0)	0 (0)	0.33 (0.31)	0 (0)	0 (0)
3	T2-QT	0.75 (0.24)	0.25 (0.24)	0.25 (0.25)	0.25 (0.24)	0.25 (0.24)
4	T2.5- QS	1 (0)	0 (0)	0 (0)	0 (0)	0 (0)
5	T2.5- QT	1 (0)	0 (0)	0 (0)	0.33 (0.31)	0.33 (0.31)
6	T2.7- QT	1 (0)	0 (0)	0 (0)	0 (0)	0 (0)
7	Floodplain-LdS	0.5 (0.38)	0 (0)	1 (0)	0.5 (0.38)	0.5 (0.38)
8	Flood-LdS1	0.75 (0.24)	0.25 (0.24)	0.25 (0.25)	0.25 (0.24)	0.25 (0.24)
9	Flood-LdS2	1 (0)	0 (0)	0.33 (0.31)	0 (0)	0 (0)
10	T2.5-QM	0.67 (0.11)	0.17 (0.09)	0.22 (0.1)	0.61 (0.12)	0.61 (0.12)
11	T2.7-QM	0.67 (0.31)	0.67 (0.31)	0.67 (0.31)	0.33 (0.31)	0.33 (0.31)

Table 4
Hydrological parameters for major perennial rivers from the Northern Atacama Desert.

Basin	Mean latitude	Area (km^2)	MAP	Mean annual runoff (m^3/s)	Runoff coefficient
Lluta	18°S 15′	3378	199[b]	1.55[b]	0.19[a]
Lauca	18°S 25′	2350	339[b]	2.07[b]	0.12[a]
San José	18°S 27′	3070	317[b]	1.28[a]	0.07[a]
Camarones	19°S 15′	4767	317[b]	0.52[a]	0.06[a]
Camiña	19°S 24′	2790	181[b]	0.61[a]	0.11[a]
Aroma	19°S 35′	1746	200[a]	0.31[a]	0.06[a]
Tarapacá	19°S 50′	1786	200[a]	0.32[a]	0.06[a]
Chacarilla	20°S 39′	1440	116[c]	0.16[a]	0.05[a]

[a] Data from JICA (1995).
[b] Data from DGA (2004, 2007).
[c] Data from Houston (2006a).

vegetation at QS to 17.6 ka (Table 1, Fig. 5). Between 15.3 and 14.6 ka, Pampa ecosystems characterized by forests of *Prosopis tamarugo* with *Distichlis spicata* (assemblage 7, Table 3) invaded the presently unvegetated western portion of the southernmost PDT basin.

Riparian ecosystems occur again at LdS between 12.1 and 11.8 ka (Fig. 5) as inferred from plant-debris in log-jam deposits (assemblage 9, Table 3). This assemblage likely represents riparian formations growing upstream from the LdS deposit. A radiocarbon date on *in situ* roots (11.8 ka, Fig. 5) found within fan deposits from the westernmost LdS canyon (Nester et al., 2007) suggests that vegetation also developed synchronously in areas downstream. By 12–11.4 ka a sparse wetland of Stipae sp (>1 km^2) developed on the T2.5 terrace at QM. Interestingly, the epidermal features of our specimens were unlike any of the present-day Stipae tribe that occurs today in northern Chile (16–28°S). Perhaps this fossil is species that became regionally extinct during pre-Hispanic times and thus has not been recorded by subsequent botanical surveys. This is not all that implausible. Palaeoecological analyses from rodent middens in the central Atacama also record the existence of locally extinct species of grasses (Latorre et al., 2002).

The latest Holocene T2.5-QM assemblage (assemblage 10, Table 3) was dominated by taxa common today in the WAC riparian and hillslope ecosystems (*Atriplex* spp, *Ch. petiolare*, *Cryptantha* sp, *Tarasa operculata*, Table 2). It also includes taxa now restricted to the higher Andes (*Euphorbia amandi* and *Junellia* sp, Table 2) and maize *Zea mays*. An important anthropogenic impact is indicated by the presence of maize and another 16 plants with a wide variety of native uses (Villagrán et al., 1999, 2003). *In situ* deposits dated to 1.01–0.71 ka were associated with abundant archeological remains such as ceramic fragments with affinities to pottery types of the Pica–Tarapacá cultural-complex (Gayo et al., 2012). Additional evidence also points to the Pica–Tarapacá culture as responsible for the transformations of QM between 1.01 and 0.71 ka (Gayo et al., 2012). Precisely, we found vestiges of an extensive transitory camp with complex irrigation channels and widespread crop fields (Fig. 9a). Other important cultural signs include cultivation and use of *Prosopis tamarugo*, introduction of extra-local plants and maize plantations (Marquet et al., 1998; Uribe, 2006).

The presence of a non-analogue formation at QM (assemblage 11, Table 3) could be due either to the prevalence of unique climate conditions or, most likely a methodological bias (Jackson and Williams, 2004). This is suggested by low taxonomic richness (n = 3 species) and by the fact that the species present are widespread within Lomas, Pampa and riparian formations. Indeed, a simultaneous record of taxa absent from Lomas (*Prosopis tamarugo*) and Pampa ecosystems (*Cistanthe* sp, Table 2) suggests a riparian modern-analogue for this assemblage.

5.2. Palaeoclimate and past hydrological change

The presence of riparian assemblages between 17.6–14.2 ka and 12.1–11.4 ka suggests major hydrologic change in the southernmost PDT basin. The lack of xerophytes and a predominance of obligate riparian taxa (*e.g. Escallonia angustifolia*, Table 2) indicate perennial riverflow and elevated groundwater tables in washes and fans that are currently

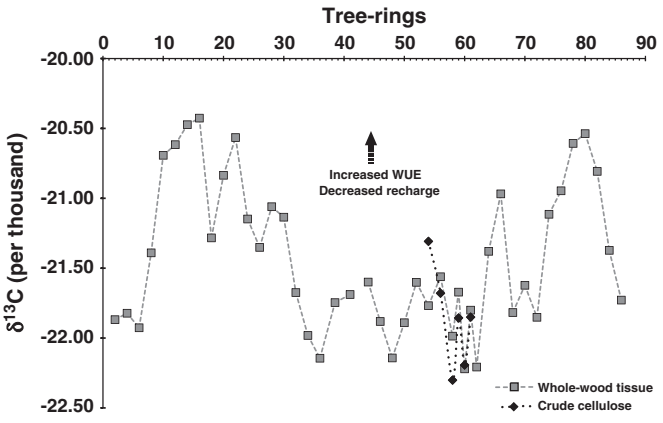

Fig. 8. $\delta^{13}C$ values for whole-tissue (gray squares) and crude cellulose (dark diamonds) in tree-rings from a *Schinus molle* fossil log dated at 15 ka (N05-12A, Table 1). The dark arrow points toward increased Water-Use Efficiency (WUE) most likely due to a decreased groundwater table.

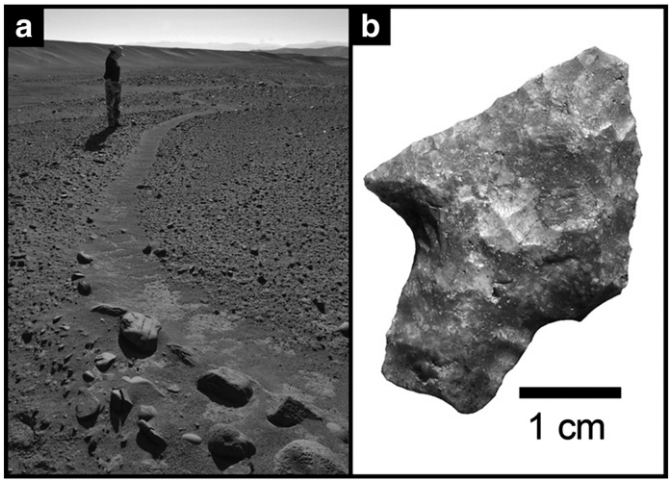

Fig. 9. Archaeological evidence for past human occupation at QM: (a) an irrigation channel dug into the T2.5 terrace. Note the stone blocks intentionally left for damming the watercourse in the foreground, (b) an undated early Archaic stemmed point from the surface of T1 at QM.

inactive or flow only occasionally. The coeval growth of a remarkably dense stand of *Prosopis tamarugo* at 15.3–14.6 ka in the distal southernmost basin also agrees with a permanent and shallow outcropping of groundwater linked to increase recharge from the adjacent eastern perennial sub-basins. Recent monitoring of natural *Prosopis tamarugo* populations in the PDT basin indicates that the vitality and growth-potential of this species increases rapidly when the water table is shallower than 13.3 mBGL (PRAMAR-DICTUC, 2007).

We interpret increased aquifer recharge and perennial riverflow in the southernmost PDT basin as a result of increased moisture availability at higher elevations in the SM. Diminished evaporation rates (an air-temperature function) and/or contribution of possible glacial melt could also be invoked as explanations for hydrological changes through time within the Longitudinal Valley south of 21°S. Late Quaternary temperature reconstructions along the central Andes are, however, controversial. First, the $\delta^{18}O$ signal in tropical Andean ice cores is affected by the so-called precipitation "amount effect" (Bradley et al., 2003; Vuille et al., 2003a, 2003b) and therefore temperature cannot be interpreted readily. Second, Equilibrium Line Altitude reconstructions based on glacier dynamics in the WAC seem to be mainly sensitive to moisture and not temperature (Zech et al., 2007, 2008; Blard et al., 2009). Indeed, climate-glacial models indicate that decreases in MAT (3°–6 °C) for glacial advances in the Bolivian Altiplano between 17 and 15 ka and ~12.5 ka were likely the result of reduced net radiation favoured by increased moisture availability and cloud cover (Clayton and Clapperton, 1997; Kull et al., 2002; Zech et al., 2007; Kull et al., 2008; Zech et al., 2008; Blard et al., 2009). Alternatively, glacier melting might have led to higher stream and groundwater discharge at PDT by increasing hydrological budgets at SM. The relative role of meltwater in ancient PDT hydrology patterns, however, must remain speculative until the glacial history of the SM is established.

Furthermore, there are three additional reasons for suspecting that increased aquifer recharge and perennial riverflow in the southernmost PDT basin most likely resulted from increased moisture availability in the SM: (1) for locations >1000 m in the WAC (Houston, 2006a), modern-day evaporation rates decrease during the wet season as a result of increased cloudiness; (2) modern perennial rivers in northernmost Chile experience peak runoff during the summer months (December–March), when precipitation and cloud cover are maximum over the Andes (Houston, 2006b, 2006c); (3) summer flooding in PDT catchments generates a significant aquifer recharge by infiltration of overflowing runoff in the alluvial fans (Houston, 2001, 2002, 2006b, 2006c).

How much precipitation would have been available to recharge the PDT aquifers and sustain perennial rivers with runoff of $\geq 0.16\ m^3/s$? Stream water sourced from rainfalls (surface runoff) in perennial rivers is a function of MAP within the headwaters, catchment area and the proportion of precipitation transmitted to river-flow. In fact, large surface runoff in the northern Atacama Desert takes place within large basins that experience high MAP in the headwaters and have elevated runoff coefficients (Table 4). To use this relation as a proxy for MAP, we computed a multi-linear regression between parameters controlling the average surface runoff (Q) in modern perennial catchments (Fig. 1, Table 4) to simulate the range of mean annual surface runoff that our latest Pleistocene rivers could have had from headwaters to mouths. The resulting relationship is:

$$Q = -1.12 - [0.00026 * A] + [0.0071 * MAP] + [11.23 * C]\left(r^2 = 0.94; F_{0.05,3,4} < 22.8; p < 0.05\right), \quad (1)$$

where A is basin area (km^2), MAP is mean annual precipitation within the headwaters region, and C a runoff coefficient. Associated past rainfall input in the headwaters was then estimated by taking the average basin area obtained from QM, QT and QS ($469\ km^2$). The runoff coefficient was considered similar to those of Quebrada Tarapacá and Chacarilla (Fig. 1, Table 4) as these have basin slopes and soil type comparable to those in the inactive southernmost PDT canyons and, most likely, similar past vegetation cover. Runoff coefficients also depend on basin area. Since the Tarapacá and Chacarilla basins are 3–4 times bigger than our basins (Table 4) we applied a correction to extrapolate the C values for our MAP estimates. This correction was made by estimating the C value for a basin of $469\ km^2$ from the existing proportional relationship between C and basin area in Tarapacá and Chacarilla basin. Thus, assuming corrected C values of 0.015 and 0.017, and using our estimated surface runoff of 2.07 and $0.16\ m^3/s$ (see Section 4.3), gives a MAP of 443 and 174 mm/yr, respectively. Today, MAP at the headwaters of these inactive canyons is ~62 mm/yr (Cebollar weather station, PRAMAR-DICTUC, 2007) therefore the hydrologic patterns at the southernmost PDT required at least a 3-fold increase in summer precipitation >3500 m in the SM between 17.6–14.2 ka and 12.1–11.4 ka.

This increase in overall MAP was probably also subject to significant variation on decadal and annual timescales, as indicated by our carbon isotope analyses on the *Schinus molle* log dated to 15 ka. Assuming a year to ring relationship, our tree-ring sequence is equivalent to an 86 yr time-series. Although multiple factors could cause variations in tree-ring ^{13}C ratios, $\delta^{13}C$ values in terrestrial plants strongly depend on atmospheric variables that affect the photosynthetic uptake of CO_2 (Farquhar et al., 1989a). Since water availability is one of the major drivers of stomatal aperture and the supply of carbon dioxide for photosynthesis in turn affects directly the RUBISCO discrimination against ^{13}C isotopes (Farquhar et al., 1989b; Leavitt and Long, 1989; Dupouey et al., 1993; Edwards et al., 2000). For that reason, several palaeoclimate studies have employed $\delta^{13}C$ in tree-rings to reconstruct past changes in relative humidity, soil water status, antecedent precipitation and/or drought stress (for a review see McCarroll and Loader, 2004). Here, we interpreted $\delta^{13}C$ changes across our record as variations in Water-Use Efficiency (WUE), which represent a proxy for changes in the carbon isotope discrimination in C_3 plants mediated by water availability (Farquhar et al., 1989b).

As *Schinus molle* is a phreatophyte (Table 2), $\delta^{13}C$ variability within the fossil log might arise from fluctuations in potential evaporation (a temperature function) and/or water table depth (function of groundwater recharge). Hydroclimatological studies in the Atacama Desert indicate that water table depth and evaporation are inversely correlated (Houston, 2006a). ENSO can exert a significant control on both parameters: El Niño (La Niña) events reduce (increase) recharge and raise (lower) evaporation along the WAC (Vuille et al., 2000; Houston, 2001, 2002, 2006a, 2006b, 2006c). Evaporation rates are linked to temperature trends, which in turn are a function of cloud cover and its effects on the net radiation. Therefore, the $\delta^{13}C$ changes in our tree-ring record likely represent variations in WUE due to fluctuations in groundwater recharge in which more positive (negative) $\delta^{13}C$ values reflect increased (decreased) WUE linked to decreased (increased) groundwater recharge. Hence, our carbon isotope analyses on the *Schinus molle* log suggest that groundwater recharge and therefore summer rainfall within the headwaters varied on decadal and annual timescales at ~15 ka (Fig. 8). This interpretation, however, must be corroborated by further studies on the modern relationship between variations in groundwater availability/depth and $\delta^{13}C$ signature in tree-rings of phreatophytes/riparian taxa from the Atacama Desert.

The $\delta^{13}C$ values show alternating periods of decreased and increased precipitation-based recharge at what are probably inter-decadal scale fluctuations; trends from tree-rings 2 to 16 suggest a period of greater recharge (rings 2–6, Fig. 8) followed by an interval of diminished water availability and increased water used efficiency (rings 8–16, Fig. 8). The decreased recharge trend continues for the following 12 rings with important variability (tree-rings 18–30, Fig. 8). A clear shift toward a period of elevated water tables occurs from rings 31 to 62 (Fig. 8). Interestingly, within this 32 ring period, intra-decadal fluctuations become much more important. Significant ring-to-ring variations (58–62 rings, Fig. 8) suggest that inter-annual changes in recharge

could be also relevant. Decrease in groundwater recharge occurs again between tree-rings 62 and 68. $\delta^{13}C$ values in tree-rings 68–72 (Fig. 8) reflect a brief pulse of increased water availability within this interval, which in turn implies that intra-decadal variation was also important. Finally, our analyses indicate that recharge decreased by tree-rings 72–80 and then sharply increased from tree-rings 80 to 86 (Fig. 8).

Occurrence of a transitional vegetation formation (assemblage 10, Table 3) in clear association with the expansion of a farming society into QM during the latest Holocene, implies that the current local hydrology and climate from the southernmost PDT changed radically again between 1.01 and 0.71 ka. The development of local agricultural practices seen at QM is dependent upon permanent irrigation (*i.e.* maize cultivation as evinced by canes dated to 0.78 ka, Table 1) argues for an augmented and sustained water supply along what is now an inactive stream. The increased hydrological budgets witnessed at QM necessary to explain both the riparian/wetland and hillslope taxa at QM would suggest either increased perennial streamflow and/or elevated local water table or a ~60-fold increase in local rainfall. We argue that such a large local precipitation increases in the PDT (where modern MAP is <1 mm/yr) or such elevated phreatic levels are likely artefacts of the record introduced by human modification of the landscape at QM. The T2.5-QM formation contains many taxa that were amply used by humans (*e.g. Euphorbia amandi*, *Junellia* sp and *Prosopis tamarugo* — see Section 5.1) (see also Gayo et al., 2012). Consequently, the preservation of T2.5-QM association and vestiges of the Pica–Tarapacá culture lead us to postulate that QM most likely experienced increased and persistent surface runoff during the latest Holocene. As there is no evidence for either reduced evaporation rates and/or increased glacial-melt input at this time, these changes must have been generated by a brief (centennial scale) increase in rainfall at higher elevations along the SM and the WAC.

5.3. Regional palaeoclimate and the Central Andean Pluvial Event (CAPE)

Diverse arrays of palaeoclimate records exist from the WAC and along the upper margin (2400–3200 m) of the Atacama Desert between 22 and 26°S. Although there are differences in timing, these records all agree in indicating that the Andean highlands (>2000 m) were much wetter than today during the last glacial–interglacial transition (Grosjean et al., 1995; Geyh et al., 1999; Betancourt et al., 2000; Bobst et al., 2001; Latorre et al., 2002; Rech et al., 2002; Latorre et al., 2003; Lowenstein et al., 2003; Rech et al., 2003a; Grosjean et al., 2005; Maldonado et al., 2005; Latorre et al., 2006; Placzek et al., 2006; Quade et al., 2008).

Recently, several researchers have identified and established the chronology of two major regional pluvial stages during the latest Pleistocene, now termed the "Central Andean (or Atacama) Pluvial Event" or CAPE (Latorre et al., 2006; Quade et al., 2008; Placzek et al., 2009). Fossil shorelines from the Uyuni basin (3700 m, ~20°S) indicate that the first stage of CAPE (CAPE I) occurred from 18 to 14.1 ka (equivalent to the Tauca lake cycle — Sylvestre et al., 1999) and was brought about by increased rainfall (Fig. 10b, Placzek et al., 2006). This ~60,000 km^2 lake provided a freshwater connection throughout the major basins of the southern Bolivian Altiplano (Placzek et al., 2006, 2009). Similar evidence comes from palaeoclimate records obtained from small endorheic basins in the Chilean Altiplano between 18° and 25°S which evince high lake levels between 15.5 and 14.0 ka (Geyh et al., 1999). Palaeowetland chronologies from the upper margin of the central Atacama Desert (>2500 m) suggest wetter conditions between 15.9 and 13.8 ka with enhanced groundwater discharge leading to elevated local water tables at Salar de Punta Negra (hereafter SPN; Quade et al., 2008) and Salar de Atacama (henceforth SDA; Rech et al., 2002; Rech et al., 2003a). High Andean steppe grasses (today confined to elevations >3600 m) migrated into what is now absolute desert (<2500 m), and summer annuals were abundant at mid-elevations (~3000 m) in rodent middens from Río Salado (~22°S) suggest a twofold increment in MAP at 17.5–16.3 ka (Latorre et al., 2006). Precipitation estimates from midden-series from the southern edge of SDA basin (~24°S, 2400 m) show a modest MAP increase at 16.2 ka (Betancourt et al., 2000; Latorre et al., 2002).

Starting at ~14.2 ka, MAP decreased to modern levels at Río Salado (Latorre et al., 2006), palaeolake Tauca collapsed abruptly (Placzek et al., 2006, 2009) and groundwater levels declined in the SPN basin (Quade et al., 2008). This widespread dry interval (also called the "Ticaña" event— Sylvestre et al., 1999) was interrupted by the onset of the second stage of the CAPE (CAPE II), which began by ~13.8 ka (Latorre et al., 2002).

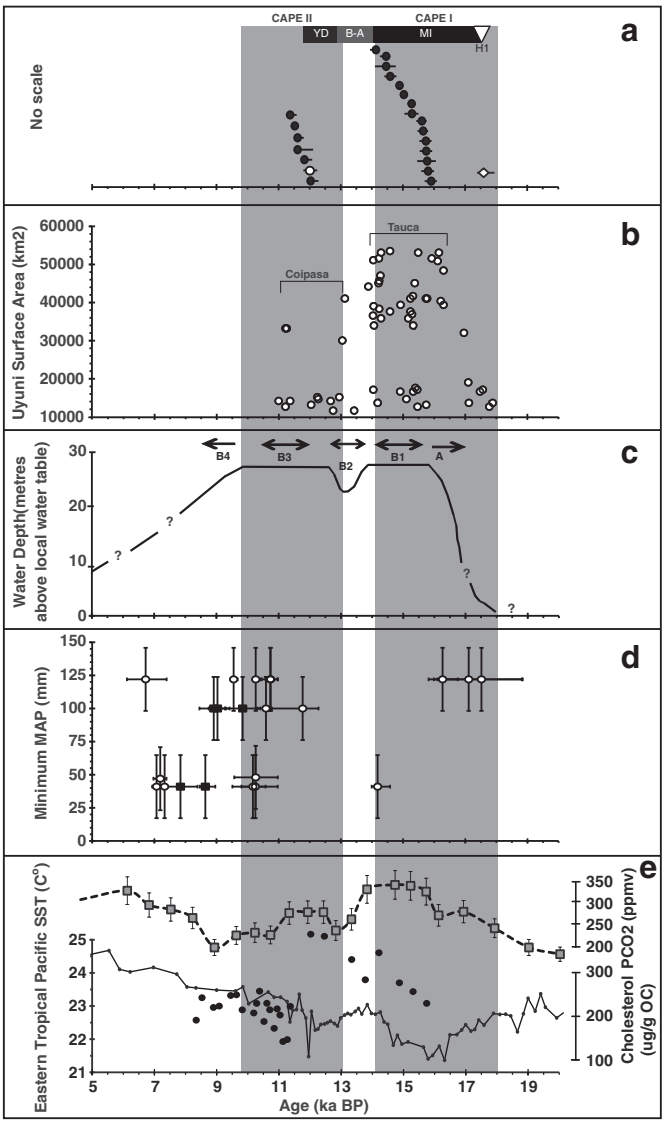

Fig. 10. Comparison of palaeoclimate records: (a) PDT fossil record, (open diamond) rhizoliths found within T2 at QS canyon (sample N05-10, Table 1), (open circle) *in situ* root preserved within fan deposits at the downstream of LdS (sample N06-11A, Table 1). H1: Heinrich Event 1, MI: the Mystery Interval, B–A: Bølling–Allerød period and YD: Younger Dryas; (b) Past lake level changes at Salar de Uyuni (Placzek et al., 2006) indicating the Tauca and Coipasa cycles. (c) Reconstructed groundwater levels from palaeowetland deposits in the central Atacama Desert, units A to B4 at SPN are discussed in Quade et al. (2008); (d) Rainfall (minimum MAP) estimates from El Sifón (open circles) and Las Juntas (dark squares) rodent-middens from Río Salado (Latorre et al., 2006); (e) inferred climate in the Equatorial Pacific for the last 20 ka, (solid-black line) Eastern Pacific SST reconstruction (core ME0005A-24; Kienast et al., 2006), (gray squares) calculated PCO_2 of Western Tropical Pacific surface-waters (core ERDC-92; Palmer and Pearson, 2003), (dark dots) down core cholesterol abundance on the Peruvian shelf (ODP Site 1228D; Makou et al., 2010). Shaded areas indicate both stages of the CAPE (Placzek et al., 2009).

The magnitude and intensity of this event differs between areas located north and south of 23°S along the Altiplano, the WAC and along the upper margin of the central Atacama Desert (Placzek et al., 2009). North of 23°S, precipitation anomalies during CAPE II appear to have been smaller than those that occurred during the first CAPE stage. Hence, a minor lake transgression ("Coipasa") is known from the Uyuni basin at ~13–11 ka (Sylvestre et al., 1999; Placzek et al., 2006, 2009). Summer rainfall increased significantly at Río Salado between 11.8 and 9.6 ka with MAP estimated to have increased from ~50 to >100 mm/yr (Latorre et al., 2006). Wet conditions have also been inferred from palaeowetland deposits dated at 13.6–10.3 ka in Quebrada Ipilla/La Higuera (~18°S, 2050 m of elevation) and at Quebrada Guataguata (20°S, 3500 m) (Rech, 2001).

CAPE II appears to have been much wetter south of 23°S, even in comparison to the preceding first CAPE stage (Placzek et al., 2009). In fact, along the WAC, lacustrine sediments from Laguna Miscanti, Lejía and Tuyajto suggest that these groundwater-fed lakes were deepest between 12.8 and 10.3 ka (Grosjean et al., 1995; Geyh et al., 1999; Grosjean et al., 2001). Rodent middens collected at SDA and SPN indicate elevated grass abundances between 12.9 and 10.5 ka (Latorre et al., 2002, 2003; Quade et al., 2008; Latorre et al., 2009) with an estimated 3-fold increase in local rainfall compared to modern values (Latorre et al., 2002, 2003, 2009). Similarly, the extent and vertical thickness of palaeowetland deposits dated at 12.7–9.7 ka imply maximum groundwater recharge and highest water tables in the SPN basin (Quade et al., 2008).

Our radiocarbon chronology of ecological and hydrological changes in the southernmost PDT basin is practically indistinguishable from the CAPE (Fig. 10). In fact, expansion of riparian ecosystems into the Longitudinal Valley along with the persistence of perennial rivers and local high water tables at 17.6–14.2 ka is synchronous with CAPE I. The PDT records correlate with the maximum highstand of the Uyuni basin throughout the Tauca lake phase at 16.4–14.1 ka (Fig. 10b), increased groundwater discharge at SPN (Fig. 10c), and enhanced rainfall at high altitudes documented from rodent middens in the central Atacama at ~22°S (Fig. 10d). Furthermore, the MAP estimates from the Río Salado midden series at 17.5–16.3 ka agree with our own precipitation estimates at SM, which account for perennial streamflow into the lower-elevation desert at ~21°S. The remarkable synchronicity of the timing and magnitude of these events also provides important information on the timing of CAPE I. Based on ten ^{14}C dates from organic-matter contained within palaeowetland sediments (B1 unit in Fig. 10c) preserved at SPN, Quade et al. (2008) state that CAPE I likely did not start before 16 ka. The evidence in the southern PDT basin and from rodent-middens (Latorre et al., 2002, 2006), however, indicates that onset of CAPE I in the Atacama Desert occurred ~17.5 ka, after the beginning of the Tauca transgression in the Uyuni basin at 18 ka (Placzek et al., 2006). Hence, the early incursion of wetter conditions at SM and along the high altitude margin of the central Atacama is consistent with the view of Placzek et al. (2009) that the chronology for CAPE should include both Altiplano lake cycles, as these reflect the immediate impact of precipitation variability. The 1500 yr delayed initiation for CAPE I at SPN (24°50′S) may reflect spatial differences in the extent of climate forcing across the northern and southern portions of the central Atacama Desert (Quade et al., 2008; Placzek et al., 2009). Alternatively, the apparent delayed onset of the CAPE I south of 23°S could also be the result of lagged response-times that characterize all groundwater-fed systems in arid regions (Tyler et al., 2006), which for the central Atacama seem to be ~500 to 1500 yrs (Rech et al., 2003a).

For the PDT, a complete lack of fossil leaf-litter deposits that date to the interval 14.2–12.1 ka could suggest that riparian ecosystems and perennial rivers retreated and local water tables dropped as headwater rainfall decreased. Our inferred onset of aridity in the SM clearly overlaps the pronounced arid phase of the CAPE between 14.2 and 13.8 ka described in other records (Fig. 10). Yet the gap in our CAPE chronology could also arise either from sampling effort or selective preservation (Gayo et al., 2012). Because the contribution of these factors cannot be totally ruled out, we are cautious of any palaeoenvironmental interpretations and implications on this hiatus must remain speculative until further geohistorical achieves from the PDT are collected and dated.

Riparian ecosystems and Stipae wetlands returned to the southernmost PDT basin between 12.1 and 11.4 ka, signifying the presence of perennial drainages during CAPE II (Fig. 10). Increased hydrological budgets at LdS and QM headwaters correlate with the Coipasa lake cycle in the Uyuni basin (Fig. 10b), the highest phreatic levels in the SPN basin (Fig. 10c) and increased summer rainfall inferred from Río Salado rodent-middens (Fig. 10d).

The limited spatial and temporal extent of our fossil leaf-litter deposits during the second stage of the CAPE, in comparison to the abundance of deposits during the first stage, can be interpreted in several ways. First, part of the reason these deposits are scarce could be due to lower MAP, which would predictably have less impact on the hydrology and biota of the southernmost PDT basin. Second, the fossil leaf-litter may be scarce due to later selective "exploitation" by local "wood hunters" during part of the XIX and toward the middle of the XX centuries for the nitrate industry and domestic demands (Briones, 1985; Hidalgo, 2009).

Whereas human intervention in the preservation of early Holocene plant-materials and those dated at 12.1–11.8 ka cannot be ruled out, there is no direct evidence to support this either. Macroscopic examination of the CAPE II materials and plant remains dated to 15.9–14.2 ka and 1.01–0.71 ka, however, indicates that independent of age, anatomical and preservation features do not differ among these three groups. North of 23°S, however, diverse palaeoclimate records appear to concur in that CAPE II was drier and shorter-lived than CAPE I (Quade et al., 2008; Placzek et al., 2009). Therefore, our limited PDT fossil record at 12.1–11.8 ka and during the early Holocene may in fact be due to the diminished spatial–temporal extent of this stage in the SM.

5.4. A major pluvial event in the Atacama Desert during the Medieval Climate Anomaly?

Our latest Holocene chronology for perennial streamflow at QM indicates that development of riparian vegetation and human settlement of the Pica–Tarapacá cultural phase occurred between 1.01 and 0.71 ka. This was apparently triggered by a wet pulse in the SM headwaters. Rodent middens and palaeowetland records from the WAC also show a brief and intense wet event dated to ~1.3–0.7 ka (Latorre et al., 2002; Rech et al., 2002; Latorre et al., 2003, 2006, 2009). A 3-fold increase in MAP has been inferred from rodent middens dated to 1.02–0.85 ka (Latorre et al., 2006, 2009).

Interestingly, there is scarce evidence for such an event on the Bolivian Altiplano. Lake records from the Titicaca basin (16°S, ~3810 m) indicate that present-day conditions have remained stable since 2 ka, with low lake-stands at 1.7–1.5 ka and 0.9–0.6 ka (Abbott et al., 1997; Binford et al., 1997; Mourguiart et al., 1998; Abbott et al., 2003; Dillehay and Kolata, 2004). Several authors have pointed out the discrepancies between the timing and climate signature of the Altiplano versus the WAC palaeoclimate records during the Holocene (*e.g.*; Betancourt et al., 2000; Grosjean, 2001; Quade et al., 2001; Latorre et al., 2002; Rech et al., 2002: Rech et al., 2003a).

Our chronology for latest Holocene climate changes in the PDT coincides with the MCA, a period between 1.05–0.6 ka marked by major hydrological change at the global scale (Stine, 1994; Graham et al., 2007, 2010). These changes were most likely driven by sustained La Niña conditions in the tropical Pacific as well as persistent positive North Atlantic Oscillation (NAO) and enhanced Atlantic Meridional Overturning Circulation (AMOC) (Graham et al., 2007, 2010; Trouet et al., 2009; Makou et al., 2010).

5.5. What drives the long-term hydrological and ecological dynamics of the PDT system?

The CAPE has been recently linked to millennial-scale variations of two different modes that today control the intra and inter-annual climate rainfall modes in the dry central Andes, the N–NE and the SE modes (Latorre et al., 2006; Quade et al., 2008; Placzek et al., 2009). These two modes differ in (1) their moisture sources; (2) drivers of inter-annual variability; and (3) spatial and/or temporal domain, often exhibiting strong antiphasing in most years (Vuille and Keimig, 2004). The N–NE mode is predominant over the tropical central Andes (15°–20°S). Associated monsoonal rainfalls are sourced from the Amazon basin (Vuille and Keimig, 2004). For this mode, inter-annual variability is modulated by SST gradients in the tropical Pacific and the intensity as well as direction of the tropical easterlies, resulting in positive (negative) precipitation anomalies during La Niña (El Niño) phase through the strengthening (weakening) and reverse flow (normal) of the easterlies (Garreaud et al., 2003; Vuille and Keimig, 2004). In contrast, the SE mode prevails along the southern central Andes (20°–30°S) with a subtropical moisture source in the Gran Chaco basin. On inter-annual scales, precipitation variability is chiefly tied to fluctuations in low-level moisture over the eastern adjacent lowlands (Vuille and Keimig, 2004).

Onset of CAPE I closely matches Heinrich Event 1 (Fig. 10a, Bond et al., 1992) and the entire event is basically identical in timing to the so-called "Mystery Interval" (17.5–14.5 ka; Denton et al., 2006). This interval marks the onset of the last global deglaciation and was characterized by a slowdown of the AMOC (McManus et al., 2004) and a southward displacement of the ITCZ (*e.g.*, Hodell et al., 2008). Biomarker records in sediment cores recovered from the Eastern Tropical Pacific (Kienast et al., 2006; Makou et al., 2010) and reconstructions of surface-water PCO_2 levels within the Western Pacific warm pool (Palmer and Pearson, 2003) indicate that CAPE I coincides with sustained La Niña-like conditions in the tropical Pacific between 18 and 14.5 ka (Fig. 10e). Hence, the strong links that exist between the Pacific SST gradients and moisture advection in the tropical central Andes, CAPE I is most likely associated with positive summer precipitation anomalies arising from the N–NE mode (Quade et al., 2008; Placzek et al., 2009). A lagged onset at SPN with only moderate increases in precipitation south of 23°S is also consistent with this interpretation (Placzek et al., 2009). Today, in the central Andes the correlation between ENSO and precipitation anomalies is stronger north of 23°S (Vuille and Keimig, 2004; Houston, 2006b). Moreover, the influence of the N–NE mode tends to decrease sharply south of 21°S, although in some years positive rainfall anomalies can reach much further south (Vuille and Keimig, 2004).

Both, the regional arid phase (14.2–13.8 ka) and the onset of CAPE II (at 13.8–13 ka) are coeval with the Bølling–Allerød interstadial (~14.5–12.7 ka, Fig. 10a), the resumption of AMOC (McManus et al., 2004) and a northward migration of the ITCZ (Hodell et al., 2008). Alkenone unsaturation SST reconstructions indicate that temperature increased by ~1.3 °C at 14–12.5 ka in the equatorial Eastern Pacific (Fig. 10e, Kienast et al., 2006). Similarly, sterol concentrations within a marine core off the central Peruvian coast show a marked reduction in cholesterol from 14.5 ka to 13.5 ka, suggesting a prevailing El Niño-like mode along the tropical Pacific (Fig. 10e, Makou et al., 2010). Sustained aridity across the central Andes from 14.2 to 13.8 ka could thus have originated in prolonged El Niño-like conditions, which today result in negative precipitation anomalies by weakening the easterly flow and moisture influx associated with the N–NE mode. Wetter conditions along WAC at 13.8–13 ka when the Tropical Pacific was locked into El Niño-like mode (Kienast et al., 2006; Makou et al., 2010) tie the beginning of CAPE II to increase moisture availability in the Gran Chaco lowlands, an important source of moisture that explains modern rainfall patterns in the southern central Andes (Placzek et al., 2009). The constrained onset for CAPE II at SDA at 13.8 ka (~24°S, Latorre et al., 2002) indeed argues for a prevailing SE mode.

Wetter conditions during CAPE II from 13 to 11.5 ka (Fig. 10a) overlap the Younger Dryas (Fig. 10a, Rasmussen et al., 2006), a partial weakening of the AMOC (McManus et al., 2004; Bakke et al., 2009) and southerly mean position of the ITZC (Haug et al., 2001; Hodell et al., 2008). Palaeoceanographic records suggest that the Tropical Pacific was characterized by a prolonged La Niña-like state between 12.2 and 11.5 ka (Fig. 10e, Palmer and Pearson, 2003; Kienast et al., 2006; Makou et al., 2010). For example, upwelling and productivity were highest at 12.2 ka, falling sharply by 11.5 ka as indicated by cholesterol abundance in an offshore marine core from Peru (Fig. 10e, Makou et al., 2010). Alkenone-based SST evolution off the western coast of tropical South America suggests significant cooling between 12.5 and 11.5 ka (Fig. 10e, Kienast et al., 2006). Surface-water PCO_2 levels indicate modest increased upwelling at the Western Tropical Pacific between 12.4 ka and 11.3 ka (Fig. 10e, Palmer and Pearson, 2003). These different lines of evidence actually point to a prevailing N–NE mode as direct casual mechanisms for increased precipitation during part of CAPE II between 13 and 11.5 ka.

In contrast, little evidence exists for La Niña-like conditions (Fig. 10e, Palmer and Pearson, 2003; Kienast et al., 2006) during the latest phase of CAPE II (after 11.5 ka) and this stage has been linked to the presence of increased moisture levels in the Gran Chaco region. The limited duration and extent of this wet phase to areas south of 23°S from 11.5 to 9.7 ka (Quade et al., 2008) agrees with this interpretation. Likewise, the limited chronological and spatial extent of the Coipasa lake cycle – a minor and short-lived transgression – in the Uyuni basin can also be explained by the fact that the N–NE mode was also less prevalent after 11.5 ka.

The similarity of timing, magnitude and intensity of the pluvial events in the PDT basin with the central Andean highlands north of 23°S, suggests that the N–NE mode can exert considerable control over the long-term dynamics of the low-elevation hydrological and ecological systems. This implies that enhanced tropical Pacific SST gradients, through its corresponding effect on the strength and direction of upper level circulation, are capable of modulating the hydrology and vegetation of the northern Atacama Desert lowlands. The fact that riparian ecosystems and higher water tables occur again in the PDT at 1.01–0.71 ka reinforces the concept that ENSO-like variability is behind these changes (see Section 5.4).

Modern hydrological change in the northern Atacama Desert is clearly linked to ENSO. During La Niña years, increased summer rainfalls along the WAC promote surface floods along ephemeral streams and increase runoff in perennial streams (often producing flooding and mudflows along the distal portions of the PDT basin), all of which results in increased aquifer recharge (Houston, 2001, 2002, 2006b, 2006c). Flooding and recharge, however, do not take place for every La Niña episode. Houston (2006b) showed that the response of these hydrological systems to ENSO variability is non-linear and that the systems exhibit high response thresholds. Significant events arise when positive summer rainfall anomalies associated with La Niña exceed 1–2 standard deviations (SD) over the average. Such events are rare, and occur sparsely every 10 to 100 years, respectively (Houston, 2006b). A high response-threshold of these hydrological systems is apparent in our reconstructions, with at least a 3-fold precipitation increase needed to establish perennial streamflow and groundwater discharge along the southernmost PDT basin. Our $\delta^{13}C$ analyses on a 15 ka *Schinus molle* log suggest that hydrologically meaningful events of increased precipitation were not sustained on inter-annual and intra/inter-decadal timescales, but rather their recurrences were likely more frequent than they are today.

The persistence of Stipae wetlands at QM (~11.4 ka) during the latest phase of CAPE indicates that long-term dynamics in the PDT could also be coupled to the SE mode. Today this mode accounts for ~30.5% of variance in summer cloudiness along the WAC from 15°

to 30°S (Vuille and Keimig, 2004). Modern links, however, between WAC streamflow, groundwater recharge and the SE mode are poorly understood. For example, despite the absence of La Niña-conditions and presence of a significant drought along the northern central Andes (Quintanilla et al., 1995), the summers of 1978–1981 were marked by major flooding in the Río Salado (Houston, 2006b). We can only speculate on the significance of water vapour content in the SE lowlands (Chaco) as a driver for hydrological change in Atacama Desert during CAPE II. The drivers of hydrological variability in the WAC could be considerably more complex than portrayed by hydroclimatologists and/or fluctuations in the SE mode could be highly relevant on longer timescales. Both hypotheses might be testable by hydroclimatology studies that incorporate palaeoclimate sensors for low-level SE moisture and long time series of Atacama river runoff.

5.6. Biogeographic consequences and cultural impacts

The Atacama Desert displays high levels of endemism, disjunct distributions between major ecosystems and overall low diversity (Arroyo et al., 1988; Rundel et al., 1991). These patterns are interpreted as the result of long-term isolation since the onset of hyperaridity during the Neogene and subsequent late Quaternary climate changes that briefly interrupted this barrier (Villagrán et al., 1983; Arroyo et al., 1988; Moreno et al., 1994).

For example, phylogenies of small mammals from the Atacama lowlands and coastal regions have been interpreted as descending from Andean populations that crossed the hyperarid landscape during the late Quaternary using east–west biotic corridors (*e.g.* Palma et al., 2005; Rodriguez-Serrano et al., 2006). Moreover, these studies specifically propose that the ancestor of coastal and lowland rodent species arrived utilizing desert riparian corridors, with populations later evolving by peripatric speciation when such corridors "closed" or became inactive. Similarly, phytogeographic analyses suggest that modern richness patterns along the WAC are partly due to the existence of riparian ecosystems that operated as "corridors" and "refuges" to Andean plants during interglacials (Arroyo et al., 1982; Villagrán et al., 1983; Arroyo et al., 1988; Luebert et al., 2009).

Palaeontological and palaeoclimatological evidence regarding the spatio-temporal dynamics of these corridors and their eventual impact on biotic dispersals has been hindered by the lack of relevant data from the low-elevation desert. Our late Quaternary record of vegetational and hydrological change in the Longitudinal Valley of northern Chile offers a missing piece toward resolving the present-day biogeographic puzzle. Our results demonstrate that riparian and wetland ecosystems from the Atacama Desert were sensitive to climate changes in the WAC, experiencing latitudinal and altitudinal changes in distributions during the course of three discrete intervals (CAPE I–II, and during the MCA) during the late Quaternary (Fig. 5). Indeed, extensive gallery forests formed within the hyperarid Longitudinal Valley during these pluvial events, harboring Andean species and facilitating biotic exchange between highlands and lowlands. These chronologically well-constrained events of vegetation expansion suggest that biogeographic corridors lasted over 3000 years during CAPE I but were rather short-lived (300 yrs or less) during CAPE II or the MCA.

Recent interdisciplinary studies suggest that past ENSO-driven environmental changes are important processes for explaining the cultural evolution and spatial–temporal dynamics of human societies in the Atacama (Williams et al., 2008; Santoro and Latorre, 2009; Santoro et al., 2011). Persistence of perennial rivers and riparian corridors along the PDT during the CAPE and the MCA would have generated attractive habitats for human colonization of the low-elevation desert. The timing of hydrological and ecological changes in the PDT basin is therefore important for understanding the peopling of western South America.

Surprisingly, very little is known regarding the impact of the CAPE on the regional archaeology. Our own preliminary finds include an undated early-style Archaic artefact found on the surface of T1 at QM, 2 km away from the latest Holocene leaf-litter deposits (Fig. 9b). This contrasts with the abundance of archaeological evidence for a significant human occupation of the low-elevation valleys during the MCA. The Pica–Tarapacá settlement at QM, initially dated to 1.01–0.71 ka clearly represents a brief but spatially extensive pulse of cultural and economic activities along southernmost PDT basin.

5.7. Implications for modern low-elevation hydrology

Currently, the PDT aquifers are under significant hydrological deficit. For reference, mean annual recharge for the total basin is ~1591 l/s (JICA, 1995; PRAMAR-DICTUC, 2007) and total groundwater outputs are >2500 l/s (Rojas and Dassargues, 2007). Excessive pumping for agriculture, industry, domestic use and mining are the primary causes of groundwater depletion in the PDT (JICA, 1995; Rojas and Dassargues, 2007; Hidalgo, 2009). Recent studies, however, argue that the PDT deficit also arises from the intermittent nature of current recharge due to inter-decadal variations in headwater rainfall and head-decay of non-renewable groundwater storage (Houston, 2001, 2002; Houston and Hart, 2004; Houston, 2006a). Several independent lines of evidence indicate that a large volume of the groundwater stored in the PDT aquifers is fossil and published ^{14}C ages range from 22 to 0.5 ka, clustering at 11.3–9.3 and 1.1–0.5 ka (Fritz et al., 1979, 1981; Magaritz et al., 1989; Aravena, 1995; JICA, 1995; Houston and Hart, 2004).

Houston and Hart (2004), however, have stated that the proportion of groundwater in the northern and central Atacama Desert considered fossil is exaggerated. They conclude that even though some aquifers are indeed non-renewable, many potential biases exist in the hydrological surveys themselves. Among these biases are: (1) a significant reservoir effect on ^{14}C dates on groundwater derived from a mixture of meteoric and thermal waters; (2) a total lack of stratification controls on the water sampling within the aquifers and/or (3) poor sampling designs across flow paths from recharge areas.

Verifying the "real" extent of fossil aquifers across the Atacama Desert will require advances in sampling strategies, increasing our knowledge of the evolution of carbon geochemistry in these waters and even achieving independent evidence for ancient recharge. It is precisely with the latter that palaeoenvironmental studies can provide potential "smoking guns" for changes in past groundwater recharge rates at different spatial–temporal scales as well as the mechanisms involved. In this context, a chronologically constrained fossil record from the southernmost PDT basin represents a tracer for massive ancient recharge of these resources. As stated previously, we have documented three distinct recharge episodes (Fig. 5). Increased regional precipitation driven by ENSO-like variability and/or fluctuations of the SE mode (see Section 5.5) augmented the activity of four tributary drainage systems of the southern PDT. Today, these contribute sporadically with less than 11% of the total basin recharge (PRAMAR-DICTUC, 2007). Multiple and coeval perennial rivers existed within QM, QT, QS and LdS with water table heights reaching near the surface in areas with present phreatic levels >70 mBGL. All of this evidence points to significant past aquifer recharge during the CAPE and the MCA.

Owing to the nature of our fossil record, we cannot assess the amount of past groundwater recharge during events (aside from the ones described here) that did not preserve on the surface of the PDT (*i.e.* a false negative). Yet, based on the assumption that past suitable conditions in the headwaters have remained relatively stable for decades, hundreds and/or thousands of years, we propose that the recharge events during the CAPE and the MCA injected important amounts of water into the PDT aquifers. The timing of latest Pleistocene groundwater recharge at the PDT was coeval with major past

recharge in the Chilean Altiplano (*e.g.* Laguna Lejía at 23°30′S; Grosjean et al., 1995). This implies that the CAPE may have led to regional formation of major fossil aquifers present throughout the central Andes and Atacama Desert.

6. Conclusions

The fossil record preserved in the southernmost PDT basin constitutes an exceptional archive of both vegetation and local hydrologic history from the hyperarid core of the Atacama Desert. This archive illuminates their response to regional climate change during the late Quaternary. Temporal correlations between changes in the PDT and other regional palaeoclimate records indicate that the long-term dynamics of these ecological and hydrological systems are closely linked to multi-millennial and centennial-scale changes in the frequency and magnitude of precipitation in the central Andes. Hence, ENSO-like variability as well as subtropical moisture changes over the Gran Chaco (*i.e.* the SE Mode of Quade et al., 2008) is a likely candidate for causal mechanisms of past hydrological change with attendant riparian and wetland invasions, as well as extirpations, in the hyperarid core of the Atacama Desert. The remarkable degree of synchronicity displayed between palaeoclimate change in the central Andean highlands and our lowland records implies that past pluvial phases in the central Andes had a lowland impact along the western Andean slope.

The hydrological and ecological changes documented here for the southernmost PDT basin during the late Quaternary have profound implications for the appraisal, management, and conservation of biological and water resources in the driest desert on Earth. Here, for the first time, we present evidence of the long-term dynamics of the riparian environments situated within the hyperarid Atacama Desert. Furthermore, past expansions/extirpations of these riparian systems constitute major contributors toward the maintenance of modern biodiversity and biogeographical patterns in the lower Atacama Desert. Similarly, we demonstrate that these coupled ecological and hydrological changes were likely key factors in determining the trajectory of human occupation of the Atacama hyperarid core.

The chronologies from the PDT and other sites from the central Andes suggest that aside from ENSO-like variability, moisture anomalies in the Gran Chaco are a major potential source for explaining regional climate variability. Our work also demonstrates that ENSO-like variability and Gran Chaco moisture changes led to three major, regional-scale recharge events during the last 18 ka in the PDT. We propose that a considerable volume of groundwater in the PDT aquifers should be treated as "fossil"; *e.g.* non-renewable resources inherited from the last glacial–interglacial cycle and the MCA. Given the importance of these fossil resources, we strongly recommend that the evaluation of groundwater potential in northern Chile takes this information into account. To develop improved water-balance models, the relationship between ancient recharge (inputs), palaeoclimate records of past headwater rainfall fluctuations, and both modes of climate variability should be incorporated.

Role of the funding source

Different aspects of this study were financed from multiple different funding sources: the Chilean Commission for Science and Technology (CONICYT – through FONDAP, FONDECYT, CIHDE and the Basal Funding Program and scholarships), the National Geographic, the National Science Foundation, and the Millennium Scientific Initiative (ICM). These funding sources had no involvement in any aspect regarding the study design, data processing and interpretation of data or either with the decision to submit this manuscript.

Disclosure statement

The authors declare no conflicts of interest.

Acknowledgments

We thank Milagros Jiménez, Daniela Osorio, Carolina Salas and Paula Ugalde for help in the field; Francisca P. Díaz-Aguirre, Francisco González, Susan Hitschfeld, Marcela Salinas and Natalia Villavicencio for their invaluable field and laboratory assistance; Antonio Maldonado (CEAZA) and Rodrigo Villa-Martínez (CEQUA) for their help in pollen identification. Paola Salgado, Matías Frugone and Pablo Masilla patiently helped with the illustrations. Patricio I. Moreno generously provided laboratory facilities for pollen analyses. Initial field study was conducted collaboratively with Nicolás Blanco of SERNAGEOMIN. Funding was provided by CONICYT #24080156 (to E.M.G), PhD scholarships from Proyecto-ICM P05-002 (to E.M.G), FONDECYT grants #1070140 and #1100916, and CIHDE (to C.M.S and C.L), National Geographic #8000-06 (to T.E.J. and C.L.), and National Science Foundation EAR-0208130 (to T.E.J.). E.M.G. and C.L. also acknowledge the ongoing support from the IEB, PFB-23 to IEB and FONDAP 1501-2001 to CASEB. Comments by Paul Wignall and two anonymous reviewers helped improve the manuscript.

Appendix A. Location, depositional features and palaeobotanical information for the 39 organic-rich deposits used in this study. Fossil fluvial terraces nomenclature according to Nester et al. (2007)

No.	Sample ID	Organic deposit	°S, °W	Terrace	Indentified taxa
Quebrada Maní (QM)					
1	QM-1	*In situ* leaf-litter	21.09, 69.28	T2.5	*Prosopis tamarugo*
2	QM-2A[a]	*In situ* canes	21.09, 69.30	T2.5	*Zea mays*
3	QM-2E[a]	*In situ* subsurface leaf-litter deposit	21.09, 69.28	T2.5	*Prosopis tamarugo*
4	QM-3[a]	*In situ* leaf-litter and wood	21.09, 69.30	T2.5	*Prosopis tamarugo*
5	QM-4[a]	*In situ* leaf-litter and wood	21.09, 69.32	T2	*Schinus molle*, *Escallonia angustifolia*
6	QM-7	*In situ* leaf-litter and wood	21.09, 69.29	T2.7	*Prosopis tamarugo*, *Cistanthe* sp
7	QM-8	*In situ* leaf-litter	21.09, 69.29	T2.7	*Cistanthe* sp, *Tessaria absinthioides*
8	QM-9	*In situ* leaf-litter and wood	21.09, 69.29	T2.7	*Prosopis tamarugo*, *Cistanthe* sp
9	QM-12	*In situ* leaf-litter and wood	21.09, 69.30	T2.5	*Prosopis tamarugo*, *Baccharis alnifolia*, *Cistanthe* sp
10	QM-13	*In situ* leaf-litter and wood	21.09, 69.31	T2.5	*Prosopis tamarugo* and *Cistanthe* sp
11	QM-14[b]	*In situ* leaf-litter	21.09, 69.31	T2.5	*Prosopis tamarugo*, *Baccharis scandens*, *Caesalpinia aphylla*, *Baccharis alnifolia*, *Atriplex* sp, *Atriplex glaucescens*, *Atriplex atacamensis*, *Cistanthe* sp, *Euphorbia amandi*, *Junellia* sp, *Tarasa operculata*, *Nicotiana longibracteata*, Solanaceae sp1, Solanaceae sp2 and *Chenopodium petiolare*
12	QM-15A	*In situ* stems	21.09, 69.30	T2.5	Stipae sp
13	QM-15B	*In situ* stems	21.09, 69.30	T2.5	Stipae sp

(*continued*)

No.	Sample ID	Organic deposit	°S, °W	Terrace	Indentified taxa
14	QM-16[b]	*In situ* leaf-litter	21.09, 69.30	T2.5	*Baccharis alnifolia*, *Tessaria absinthioides*, *Cortaderia atacamensis*, *Muhlenbergia* sp, *Polypogon interruptus*, *Prosopis tamarugo*, *Atriplex atacamensis*, *Caesalpinia aphylla*, *Cistanthe* sp and *Cryptantha* sp
15	QM-17	*In situ* stems	21.09, 69.30	T2.5	Stipae sp
16	QM-18[b]	*In situ* leaf-litter	21.09, 69.30	T2.5	*Prosopis tamarugo*
17	QM-19	*In situ* stems	21.09, 69.30	T2.5	Stipae sp
Quebrada Sipuca (QS)					
18	QS-1[a]	*In situ* leaf-litter and wood	21.23, 69.19	T2	*Schinus molle* and *Escallonia angustifolia*
19	QS-2[a]	*In situ* indurated leaf-litter	21.23, 69.20	T2	*Escallonia angustifolia*, Poaceae sp and *Prosopis tamarugo*
20	QS-3[a]	*In situ* leaf-litter and wood	21.23, 69.20	T2.5	*Schinus molle* and *Escallonia angustifolia*
Quebrada Tambillo (QT)					
21	QT-1[a]	*In situ* leaf-litter	21.43, 69.25	T2	*Escallonia angustifolia*
22	QT-2[a]	*In situ* indurated leaf-litter	21.43, 69.25	T2	*Escallonia angustifolia*, *Schinus molle*, Asteraceae sp, Poaceae sp and *Prosopis tamarugo*
23	QT-3	*In situ* leaf-litter	21.43, 69.25	T2	*Escallonia angustifolia*, *Schinus molle* and *Cistanthe* sp
24	QT-5[a]	*In situ* leaf-litter	21.43, 69.25	T2.7	*Schinus molle* and *Escallonia angustifolia*
25	QT-6[a]	*In situ* subsurface leaf-litter deposit	21.43, 69.25	T2.5	*Schinus molle* and *Escallonia angustifolia*
26	QT-7	*In situ* leaf-litter and wood	21.44, 69.26	T2.7	*Escallonia angustifolia*
27	QT-8[a]	*In situ* subsurface leaf-litter deposit	21.44, 69.26	T2.7	*Baccharis scandens* and *Schinus molle*
28	QT-9[a]	*In situ* leaf-litter and grasses	21.44, 69.31	T2.5	*Escallonia angustifolia*, *Schinus molle* and *Cortaderia atacamensis*
29	N05-11[a]	Log	21.44, 69.25	T2.5	*Schinus molle*
Lomas de Sal (LdS)					
30	LdS-1[a]	Plant debris	21.39, 69.42	Flood deposit	*Schinus molle* and *Escallonia angustifolia*
31	LdS-4	Plant debris	21.40, 69.44	Flood deposit	*Schinus molle* and *Escallonia angustifolia*
32	LdS-5	*In situ* leaf-litter and wood	21.40, 69.44	Alluvial floodplains	*Caesalpinia aphylla*, *Escallonia angustifolia*, *Tessaria absinthioides* and *Schinus molle*
33	LdS-6A	Plant debris	21.40, 69.44	Flood deposit	*Prosopis tamarugo* and *Cistanthe* sp
34	LdS-6B	Plant debris	21.40, 69.44	Flood deposit	*Prosopis tamarugo*
35	LdS-7	*In situ* leaf-litter, grasses and wood	21.43, 69.46	Alluvial floodplains	*Prosopis tamarugo* and *Distichlis spicata*
36	LdS-8	*In situ* leaf-litter, grasses and wood	21.43, 69.46	Alluvial floodplains	*Prosopis tamarugo* and *Distichlis spicata*
37	N04-14A[a]	Plant debris	21.40, 69.42	Flood deposit	*Schinus molle* and *Escallonia angustifolia*
38	N05-12A[a]	Log	21.40, 69.42	Flood deposit	*Schinus molle*
39	N05-18[a]	Log	21.40, 69.43	Flood deposit	*Schinus molle*

[a]Previously reported in Nester et al. (2007).
[b]Previously reported in Gayo et al. (2012).

References

Abbott, M.B., Seltzer, G.O., Kelts, K.R., Southon, J., 1997. Holocene paleohydrology of the tropical Andes from lake records. Quaternary Research 47, 70–80.

Abbott, M.B., Wolfe, B.B., Wolfe, A.P., Seltzer, G.O., Aravena, R., Mark, B.G., Polissar, P.J., Rodbell, D.T., Rowe, H.D., Vuille, M., 2003. Holocene paleohydrology and glacial history of the central Andes using multiproxy lake sediment studies. Palaeogeography, Palaeoclimatology, Palaeoecology 194, 123–138.

Aravena, R., 1995. Isotope hydrology and geochemistry of northern Chile groundwaters. Bulletin de l'Institut français d'études andines 24, 495–503.

Arroyo, M.T.K., Villagrán, C., Marticorena, C., Armesto, J.J., 1982. Flora y relaciones biogeograficas en los Andes del norte de Chile (18–19 degrees S). In: Veloso, A., Bustos, E. (Eds.), El Ambiente Natural y las Poblaciones Humanas de los Andes del Norte Grande de Chile (Arica, Lat. 18 28′ S). Rostlac, Montevideo, pp. 71–92.

Arroyo, M.T.K., Squeo, F.A., Armesto, J., Villagrán, C., 1988. Effects of aridity on plant diversity in the northern Chilean Andes: results of a natural experiment. Annals of the Missouri Botanical Garden 75, 55–78.

Baker, P.A., Rigsby, C.A., Seltzer, G.O., Fritz, S.C., Lowenstein, T.K., Bacher, N.P., Veliz, C., 2001. Tropical climate changes at millennial and orbital timescales on the Bolivian Altiplano. Nature 409, 698–701.

Bakke, J., Lie, O., Heegaard, E., Dokken, T., Haug, G.H., Birks, H.H., Dulski, P., Nilsen, T., 2009. Rapid oceanic and atmospheric changes during the Younger Dryas cold period. Nature Geoscience 2, 202–205.

Betancourt, J.L., Latorre, C., Rech, J., Quade, J., Rylander, K.A., 2000. A 22,000-yr record of monsoonal precipitation from northern Chile's Atacama Desert. Science 289, 1546–1550.

Binford, M.W., Kolata, A.L., Brenner, M., Janusek, J.W., Seddon, M.T., Abbott, M., Curtis, J.H., 1997. Climate variation and the rise and fall of an Andean civilization. Quaternary Research 47, 235–248.

Blard, P.H., Lavé, J., Farley, K.A., Fornari, M., Jiménez, N., Ramirez, V., 2009. Late local glacial maximum in the Central Altiplano triggered by cold and locally-wet conditions during the paleolake Tauca episode (17–15 ka, Heinrich 1). Quaternary Science Reviews 28, 3414–3427.

Bobst, A.L., Lowenstein, T.K., Jordan, T.E., Godfrey, L.V., Hein, M.C., Ku, T.-L., Luo, S., 2001. A 106 ka paleoclimate record from drill core of the Salar de Atacama, northern Chile. Palaeogeography, Palaeoclimatology, Palaeoecology 173, 21–42.

Bond, G., Heinrich, H., Broecker, W.S., Labeyrie, L., McManus, J., Andrews, J., Huon, S., Jantschik, R., Clasen, S., Simet, C., Tedesco, K., Klas, M., Bonani, G., Ivy, S., 1992. Evidence for massive discharges of icebergs into the North Atlantic during the last glacial period. Nature 360, 245–249.

Bradley, R.S., Vuille, M., Hardy, D., Thompson, L.G., 2003. Low latitude ice cores record Pacific sea surface temperatures. Geophysical Research Letters 30, 1174–1177.

Briones, L., 1985. Visión retrospectiva antropogenica del *Prosopis*. In: Habit, M.A. (Ed.), Estado actual del conocimiento sobre *Prosopis tamarugo*. FAO, Arica-Chile.

Cane, M., Clement, A.C., 1999. A role for the tropical Pacific coupled ocean–atmosphere system on Milankovitch and millennial timescales. Part II: global impacts. In: Clark, P.U., Webb, R.S., Keigwin, L.D. (Eds.), Mechanisms of global climate change at millennial time scales. Geophysical Monograph. American Geophysical Union, Washington D.C., pp. 373–383.

Cereceda, P., Larrain, H., Osses, P., Farías, M., Egaña, I., 2008. The climate of the coast and fog zone in the Tarapacá Region, Atacama Desert, Chile. Atmospheric Research 87, 301–311.

Clayton, J.D., Clapperton, C.M., 1997. Broad synchrony of a Late-glacial glacier advance and the highstand of palaeolake Tauca in the Bolivian Altiplano. Journal of Quaternary Science 12, 169–182.

Clement, A., Cane, M., 1999. A role for the Tropical Pacific coupled ocean–atmosphere system on Milankovitch and millennial timescales. Part I: a modeling study of tropical Pacific variability. In: Clark, P.U., Webb, R.S., Keigwin, L.D. (Eds.), Mechanisms of Global

Climate Change at Millennial Time Scales. Geophysical Monograph Series, Washington, DC, pp. 363–372.
Clement, A.C., Seager, R., Cane, M.A., 1999. Orbital controls on the El Niño/Southern Oscillation. Paleoceanography 14, 441–456.
Covarrubias, R., Toro, H., Villaseñor, R., Chiappa, E., Mellado, I., 1994. Caída de materiales desde la copa de *Prosopis tamarugo* Phil, en la Pampa del Tamarugal. I Región, Chile. Bosque 15, 39–49.
Denton, G.H., Broecker, W.S., Alley, R.B., 2006. The mystery interval 17.5 to 14.5 kyrs ago. PAGES News 14, 14–16.
DGA, 1987. Balance Hídrico Nacional. Ministerio de Obras Públicas, Santiago-Chile, p. 150.
DGA, 2004. Informe Final: Diagnóstico y clasificación de los cursos y cuerpos de agua según objetivos de calidad. In: MOP (Ed.), Ministerio de Obras Públicas, Santiago, Chile, p. 362.
DGA, 2007. Informe Final: Estimaciones de demanda de agua y proyecciones futuras. Zona I Norte. Regiones I a IV. In: MOP (Ed.), Ministerio de Obras Públicas, Santiago-Chile, p. 596.
DGF, 2007. Estudio de Variabilidad Climática en Chile para el Siglo XXI financiado por la Comisión Nacional de Medio Ambiente (CONAMA). Departamento de Geofísica, Universidad de Chile. http://www.dgf.uchile.cl/PRECIS.
Dillehay, T.D., Kolata, A.L., 2004. Long-term human response to uncertain environmental conditions in the Andes. Proceedings of the National Academy of Sciences 101, 4325–4330.
Dupouey, J.L., Leavitt, S., Choisnel, E., Jourdain, S., 1993. Modelling carbon isotope fractionation in tree rings based on effective evapotranspiration and soil water status. Plant, Cell & Environment 16, 939–947.
Edwards, T.W.D., Graf, W., Trimborn, P., Stichler, W., Lipp, J., Payer, H.D., 2000. d13C response surface resolves humidity and temperature signals in trees. Geochimica et Cosmochimica Acta 64, 161–167.
Ewing, S.A., Sutter, B., Owen, J., Nishizumi, K., Sharp, W., Cliff, S.S., Perry, K., Dietrich, W., McKay, C.P., Amundson, R., 2006. A threshold in soil formation at Earth's arid–hyperarid transition. Geochimica et Cosmochimica Acta 70, 5293–5322.
Faegri, K., Iversen, J., 1989. Textbook of Pollen Analysis. John Willey & Sons, London-UK.
Farquhar, G.D., Ehleringer, J.R., Hubick, K.T., 1989a. Carbon isotope discrimination and photosynthesis. Annual Review of Plant Biology 40, 503–537.
Farquhar, G.D., Hubick, K.T., Condon, A.G., Richards, R.A., 1989b. Carbon isotope fractionation and plant water-use efficiency. In: Rundel, P.W., Ehleringer, J.R., Nagy, K.A. (Eds.), Stable Isotopes in Ecological Research. Springer-Verlag, New York, pp. 21–40.
Fritz, P., Hennings, C.S., Suzuki, O., Salati, E., 1979. Isotope hydrology in Northern Chile. Isotope Hydrology 1978. IAEA-228/26-SM, Vienna-Austria, pp. 525–544.
Fritz, P., Suzuki, O., Silva, C., Salati, E., 1981. Isotope hydrology of groundwaters in the Pampa del Tamarugal, Chile. Journal of Hydrology 53, 161–184.
Fritz, S.C., Baker, P.A., Lowenstein, T.K., Seltzer, G.O., Rigsby, C.A., Dwyer, G.S., Tapia, P.M., Arnold, K.K., Ku, T.-L., Luoh, S., 2004. Hydrologic variation during the last 170,000 years in the southern hemisphere tropics of South America. Quaternary Research 61, 95–104.
Gajardo, R., 1994. La vegetación natural de Chile: clasificación y distribución geográfica. Editorial Universitaria, Santiago-Chile.
Garreaud, R.D., 1999. Multiscale analysis of the summertime precipitation over the central Andes. Monthly Weather Review 127, 901–921.
Garreaud, R.D., Vuille, M., Clement, A., 2003. The climate of the Altiplano: observed current conditions and mechanisms of past changes. Palaeogeography, Palaeoclimatology, Palaeoecology 194, 5–22.
Gayo, E.M., Latorre, C., Santoro, C.M., Maldonado, A., De Pol-Holz, R., 2012. Hydroclimate variability in the low-elevation Atacama Desert over the last 2500 years. Climate of the Past 8, 287–306.
Geyh, M.A., Grosjean, M., Núñez, L., Schotterer, U., 1999. Radiocarbon reservoir effect and the timing of the late-Glacial/Early Holocene humid phase in the Atacama Desert (northern Chile). Quaternary Research 52, 143–153.
González, F.J., 2008. Evolución del tamaño corporal en roedores en el Desierto de Atacama durante los últimos 40.000 años. Unpublished Bachelor's degree thesis, Pontificia Universidad Católica de Chile.
Graham, N.E., Hughes, M.K., Ammann, C.M., Cobb, K.M., Hoerling, M.P., Kennett, D.J., Kennett, J.P., Rein, B., Stott, L., Wigand, P.E., Xu, T., 2007. Tropical Pacific — mid-latitude teleconnections in medieval times. Climatic Change 83, 241–285.
Graham, N.E., Ammann, C.M., Fleitmann, D., Cobb, K.M., Luterbacher, J., 2010. Support for global climate reorganization during the "Medieval Climate Anomaly". Climate Dynamics 37, 1217–1245.
Grosjean, M., 2001. Mid-Holocene climate in the south-central Andes: humid or dry? Science 292, 2391a.
Grosjean, M., Geyh, M.A., Messerli, B., Schotterer, U., 1995. Late-glacial and early Holocene lake sediments, ground-water formation and climate in the Atacama Altiplano 22–24°S. Journal of Paleolimnology 14, 241–252.
Grosjean, M., van Leeuwen, J.F.N., van der Knaap, W.O., Geyh, M.A., Ammann, B., Tanner, W., Messerli, B., Núñez, L.A., Valero-Garcés, B.L., Veit, H., 2001. A 22,000 ^{14}C year BP sediment and pollen record of climate change from Laguna Miscanti (23° S), northern Chile. Global and Planetary Change 28, 35–51.
Grosjean, M., Núñez, L., Cartajena, I., 2005. Paleoindian occupaton in the Atacama Desert, Northern Chile. Journal of Quaternary Science 20, 643–653.
Gutierrez, J.R., López-Cortes, F., Marquet, P.A., 1998. Vegetation in an altitudinal gradient along the Río Loa in the Atacama Desert of northern Chile. Journal of Arid Environments 40, 383–399.
Haug, G.H., Hughen, K.A., Sigman, D.M., Peterson, L.C., Röhl, U., 2001. Southward migration of the intertropical convergence zone through the Holocene. Science 293, 1304–1308.
Hidalgo, J., 2009. Civilización y fomento: La "Descripción de Tarapacá" de Antonio O'Brien, 1765. Chungara Revista de Antropología Chilena 41, 5–44.
Hodell, D.A., Anselmetti, F.S., Ariztegui, D., Brenner, M., Curtis, J.H., Gilli, A., Grzesik, D.A., Guilderson, T.J., Müller, A.D., Bush, M.B., Correa-Metrio, A., Escobar, J., Kutterolf, S., 2008. An 85-ka record of climate change in lowland Central America. Quaternary Science Reviews 27, 1152–1165.
Hoke, G.D., Isacks, B.L., Jordan, T.E., Yu, J.S., 2004. Groundwater-sapping origin for the giant quebradas of northern Chile. Geology 32, 605–608.
Houston, J., 2001. La precipitación torrencial del año 2000 en Quebrada Chacarilla y el cálculo de recarga al acuífero Pampa Tamarugal, norte de Chile. Revista Geológica de Chile 28, 163–177.
Houston, J., 2002. Groundwater recharge through an alluvial fan in the Atacama Desert, northern Chile: mechanisms, magnitudes and causes. Hydrological Processes 16, 3019–3035.
Houston, J., 2006a. Evaporation in the Atacama Desert: an empirical study of spatio-temporal variations and their causes. Journal of Hydrology 330, 402–412.
Houston, J., 2006b. The great Atacama flood of 2001 and its implications for Andean hydrology. Hydrological Processes 20, 591–610.
Houston, J., 2006c. Variability of precipitation in the Atacama Desert: its causes and hydrological impact. International Journal of Climatology 26, 2181–2198.
Houston, J., Hart, D., 2004. Theoretical head decay in closed basin aquifers: an insight into fossil groundwater and recharge events in the Andes of northern Chile. Quarterly Journal of Engineering Geology & Hydrogeology 37, 131–139.
Houston, J., Hartley, A.J., 2003. The central Andean west-slope rainshadow and its potential contribution to the origin of hyper-aridity in the Atacama Desert. International Journal of Climatology 23, 1453–1464.
Jackson, S.T., Williams, J.W., 2004. Modern analogs in Quaternary Paleoecology: here today, gone yesterday, gone tomorrow? Annual Review of Earth and Planetary Sciences 32, 495–537.
JICA, 1995. The Study on the Development of Water Resources in Northern Chile. In: JICA-PCI (Ed.), , p. 249. Tokyo, Japan.
Kienast, M., Kienast, S.S., Calvert, S.E., Eglinton, T.I., Mollenhauer, G., François, R., Mix, A.C., 2006. Eastern Pacific cooling and Atlantic overturning circulation during the last deglaciation. Nature 443, 846–849.
Kuch, M., Rohland, N., Betancourt, J., Latorre, C., Steppan, S., Poinar, H., 2002. Molecular analysis of an 11,700-year old rodent midden from the Atacama Desert, Chile. Molecular Ecology 11, 913–924.
Kull, C., Grosjean, M., Veit, H., 2002. Modeling modern and Late Pleistocene glacioclimatological conditions in the North Chilean Andes (29–30°). Climatic Change 52, 359–381.
Kull, C., Imhof, S., Grosjean, M., Zech, R., Veit, H., 2008. Late Pleistocene glaciation in the Central Andes: temperature versus humidity control — a case study from the eastern Bolivian Andes (17°S) and regional synthesis. Global and Planetary Change 60, 148–164.
Lanino, M., 2004. Antecedentes climáticos de la Estación Experimental Canchones, en la Pampa del Tamarugal. Revista de Agricultura del Desierto 3, 1–24.
Latorre, C., Betancourt, J.L., Rylander, K.A., Quade, J., 2002. Vegetation invasions into absolute desert: a 45,000-yr rodent midden record from the Calama–Salar de Atacama Basins, northern Chile (22–24° S). Geological Society of America Bulletin 114, 349–366.
Latorre, C., Betancourt, J.L., Rylander, K.A., Quade, J., Matthei, O., 2003. A vegetation history from the arid prepuna of northern Chile (22–23° S) over the last 13,500 years. Palaeogeography, Palaeoclimatology, Palaeoecology 194, 223–246.
Latorre, C., Betancourt, J.L., Rech, J.A., Quade, J., Holmgren, C., Placzek, C., Maldonado, A., Vuille, M., Rylander, K.A., 2005. Late Quaternary history of the Atacama Desert. In: Smith, M., Hesse, P. (Eds.), 23° S: The Archaeology and Environmental History of the Southern Deserts. National Museum of Australia Press, Canberra, Australia, pp. 73–90.
Latorre, C., Betancourt, J.L., Arroyo, M.T.K., 2006. Late Quaternary vegetation and climate history of a perennial river canyon in the Río Salado basin (22°S) of Northern Chile. Quaternary Research 65, 450–466.
Latorre, C., González, F.J., Rojas, M., Houston, J., 2009. Estimaciones cuantitativas de precipitaciones para los últimos 14.000 años en el Desierto de Atacama a partir de paleomadrigueras de roedores. XII Congreso Geológico Chileno, pp. 1–4. Santiago-Chile.
Leavitt, S.W., Long, A., 1989. Drought indicated in carbon-13/carbon-12 ratios of southwestern tree rings. Journal of the American Water Resources Association 25, 341–347.
Lioubimtseva, E., 2004. Climate change in arid environments: revisiting the past to understand the future. Progress in Physical Geography 28, 502–530.
Lowenstein, T.K., Hein, M.C., Bobst, A.L., Jordan, T.E., Ku, T.-L., Luo, S., 2003. An assessment of stratigraphic completeness in climate-sensitive closed-basin lake sediments: Salar de Atacama, Chile. Journal of Sedimentary Research 73, 91–104.
Luebert, F., Pliscoff, P., 2006. Sinopsis bioclimática y vegetacional de Chile. Editorial Universitaria, Santiago.
Luebert, F., Wen, J.U.N., Dillon, M.O., 2009. Systematic placement and biogeographical relationships of the monotypic genera *Gypothamnium* and *Oxyphyllum* (Asteraceae: Mutisioideae) from the Atacama Desert. Botanical Journal of the Linnean Society 159, 32–51.
Macfarlane, C., Warren, C.R., White, D.A., Adams, M.A., 1999. A rapid and simple method for processing wood to crude cellulose for analysis of stable carbon isotopes in tree rings. Tree Physiology 19, 831–835.
Magaritz, M., Aravena, R., Peña, H., Suzuki, O., Grilli, A., 1989. Water chemistry and isotope study of streams and springs in northern Chile. Journal of Hydrology 108, 323–341.
Magaritz, M., Aravena, R., Peña, H., Suzuki, O., Grilli, A., 1990. Source of ground water in the Deserts of Northern Chile: evidence of deep circulation of ground water from the Andes. Ground Water 28, 513–517.
Makou, M.C., Eglinton, T.I., Oppo, D.W., Hughen, K.A., 2010. Postglacial changes in El Niño and La Niña behavior. Geology 38, 43–46.
Maldonado, A., Betancourt, J.L., Latorre, C., Villagrán, C., 2005. Pollen analyses from a 50,000-yr rodent midden series in the southern Atacama Desert (25°30′S). Journal of Quaternary Science 20, 493–507.

Marquet, P.A., Bozinovic, F., Bradshaw, G.A., Cornelius, C., Gonzalez, H., Gutierrez, J.R., Hajek, E.R., Lagos, J.A., Lopez-Cortés, F., Nuñez, L., Rosello, E.F., Santoro, C., Samaniego, H., Standen, V.G., Torres-Mura, J.C., Jaksic, F.M., 1998. Los ecosistemas del Desierto de Atacama y área andina adyacente en el norte de Chile. Revista Chilena de Historia Natural 71, 593–617.

Martin, L., Bertaux, J., Correge, T., Ledru, M.-P., Mourguiart, P., Sifeddine, A., Soubies, F., Wirrmann, D., Suguio, K., Turcq, B., 1997. Astronomical forcing on contrasting rainfall changes in tropical South America between 12,400 and 8,800 cal yr B.P. Quaternary Research 47, 117–122.

Matthei, O., 1965. Estudio crítico de las gramíneas del género *Stipa* en Chile. Gayana, Botánica 13, 3–137.

McCarroll, D., Loader, N.J., 2004. Stable isotopes in tree rings. Quaternary Science Reviews 23, 771–801.

McManus, J.F., Francois, R., Gherardi, J.M., Keigwin, L.D., Brown-Leger, S., 2004. Collapse and rapid resumption of Atlantic meridional circulation linked to deglacial climate changes. Nature 428, 834–837.

Moreno, P.I., Villagrán, C., Marquet, P.A., Marshall, L.G., 1994. Quaternary paleobiogeography of northern and central Chile. Revista Chilena de Historia Natural 67, 487–502.

Mourguiart, P., Correge, T., Wirrmann, D., Argollo, J., Montenegro, M.E., Pourchet, M., Carbonel, P., 1998. Holocene palaeohydrology of Lake Titicaca estimated from an ostracod-based transfer function. Palaeogeography, Palaeoclimatology, Palaeoecology 143, 51–72.

Muñoz-Pizarro, C., 1966. Sinopsis de la flora chilena: Claves para la identificación de familias y géneros. Ediciones Universidad de Chile, Santiago-Chile.

Nester, P.L., Gayo, E., Latorre, C., Jordan, T.E., Blanco, N., 2007. Perennial stream discharge in the hyperarid Atacama Desert of northern Chile during the latest Pleistocene. Proceedings of the National Academy of Sciences 104, 19724–19729.

Nicora, E.G., Rúgolo de Agrasar, Z.E., 1987. Los géneros de gramíneas de America Austral. Editorial Hemisferio Sur, Buenos Aires-Argentina.

Palma, R.E., Marquet, P.A., Boric-Bargetto, D., 2005. Inter- and intraspecific phylogeography of small mammals in the Atacama Desert and adjacent areas of northern Chile. Journal of Biogeography 32, 1931–1941.

Palmer, M.R., Pearson, P.N., 2003. A 23,000-year record of surface water pH and PCO_2 in the Western Equatorial Pacific Ocean. Science 300, 480–482.

Placzek, C., Quade, J., Patchett, P.J., 2006. Geochronology and stratigraphy of Late Pleistocene lake cycles on the Southern Bolivian Altiplano: implications for causes of tropical climate change. Geological Society of America Bulletin 118, 515–532.

Placzek, C., Quade, J., Betancourt, J.L., Patchett, P.J., Rech, J.A., Latorre, C., Matmon, A., Holmgren, C., English, N.B., 2009. Climate in the dry central Andes over geologic, millennial, and interannual timescales. Annals of the Missouri Botanical Garden 96, 386–397.

PRAMAR-DICTUC, 2007. Estudio de Impacto Ambiental: Proyecto Minero Soronal. SQM S.A, Santiago-Chile, p. 500.

Quade, J., Rech, J., Betancourt, J., Latorre, C., 2001. Mid-Holocene climate in the south-central Andes: humid or dry? Science 292, 2391a.

Quade, J., Rech, J.A., Betancourt, J.L., Latorre, C., Quade, B., Rylander, K.A., Fisher, T., 2008. Paleowetlands and regional climate change in the central Atacama Desert, northern Chile. Quaternary Research 69, 343–360.

Quintanilla, J., Coudrain-Ribstein, A., Martínez, J., Camacho, V., 1995. Hidroquímica de las aguas del Altiplano de Bolivia. Bulletin de l'Institut Français d'études Andines 24, 461–471.

Rasmussen, S.O., Andersen, K.K., Svensson, A.M., Steffensen, J.P., Vinther, B.M., Clausen, H.B., Siggaard-Andersen, M.L., Johnsen, S.J., Larsen, L.B., Dahl-Jensen, D., Bigler, M., Röthlisberger, R., Fischer, H., Goto-Azuma, K., Hansson, M.E., Ruth, U., 2006. A new Greenland ice core chronology for the last glacial termination. Journal of Geophysical Research 111.

R-Development-Core-Team, 2008. R: A Language and Environment for Statistical Computing. R Foundation for Statistical Computing, Vienna, Austria.

Rech, J.A., 2001. Late Quaternary paleohydrology and surficial processes of the Atacama Desert, Chile: evidence from wetlands deposits and stable isotopes of soil salts. The University of Arizona.

Rech, J., Quade, J., Betancourt, J.L., 2002. Late Quaternary paleohydrology of the central Atacama Desert (22–24° S), Chile. Geological Society of America Bulletin 114, 334–348.

Rech, J., Pigati, J.S., Quade, J., Betancourt, J.L., 2003a. Re-evaluation of mid-Holocene wetland deposits at Quebrada Puripica, northern Chile. Palaeogeography, Palaeoclimatology, Palaeoecology 194, 207–222.

Rech, J.A., Quade, J., Hart, W.S., 2003b. Isotopic evidence for the origin of Ca and S in soil gypsum, anhydrite, and calcite in the Atacama Desert, Chile. Geochimica et Cosmochimica Acta 67, 575–586.

Rodriguez-Serrano, E., Cancino, R.A., Palma, R.E., 2006. Molecular phylogeography of *Abrothrix olivaceus* (Rodentia: Sigmodontinae) in Chile. Journal of Mammalogy 87, 971–980.

Rojas, R., Dassargues, A., 2007. Groundwater flow modelling of the regional aquifer of the Pampa del Tamarugal, northern Chile. Hydrogeology Journal 15, 537–551.

Rundel, P.W., Dillon, M.O., Palma, B., Mooney, H.A., Gulmon, S.L., Ehleringer, J.R., 1991. The phytogeography and ecology of the Coastal Atacama and Peruvian Deserts. Aliso 13, 1–49.

Santoro, C.M., Latorre, C., 2009. Propuesta metodológica interdisciplinaria para poblamientos humanos Pleistoceno tardío/Holoceno temprano, precordillera de Arica, Desierto de Atacama Norte. Andes 7, 13–35.

Santoro, C.M., Latorre, C., Salas, C., Osorio, D., Ugalde, P., Jackson, D., Gayo, E.M., 2011. Ocupación Humana pleistocénica en el Desierto de Atacama. Primeros resultados de la aplicación de un modelo predictivo interdisciplinario. Chungara Revista de Antropología Chilena 43, 353–366.

Stine, S., 1994. Extreme and persistent drought in California and Patagonia during Mediaeval time. Nature 369, 546–549.

Sylvestre, F., Servant, M., Servant-Vildary, S., Causse, C., Fournier, M., Ybert, J.-P., 1999. Lake-level chronology on the Southern Bolivian Altiplano (18°–23°S) during late-glacial time and the early Holocene. Quaternary Research 51, 54–66.

Tomlinson, A.J., Blanco, N., Maksaev, V., Dilles, J., Grunder, A.L., Ladino, M., 2001. Geología de la Precordillera Andina de Quebrada Blanca-Chuquicamata, Regiones I y II (20°30′–22°30′S). Servicio Nacional de Geología y Minería, Santiago-Chile, pp. 1–444.

Trouet, V., Esper, J., Graham, N.E., Baker, A., Scourse, J.D., Frank, D.C., 2009. Persistent positive North Atlantic Oscillation mode dominated the Medieval Climate Anomaly. Science 324, 78–80.

Tyler, S.W., Muñoz, J.F., Wood, W.W., 2006. The response of playa and sabkha hydraulics and mineralogy to climate forcing. Ground Water 44, 329–338.

Uribe, M., 2006. Acerca de complejidad, desigualdad social y el complejo cultural Pica–Tarapacá en los Andes Centro-Sur (1000–1450 DC). Estudios Atacameños 31, 91–114.

Villagrán, C., Arroyo, M.T.K., Marticorena, C., 1983. Efectos de la desertización en la distribución de la flora andina de Chile. Revista Chilena de Historia Natural 56, 137–157.

Villagrán, C., Castro, V., Sánchez, G., Hinojosa, F.L., Latorre, C., 1999. La tradición altiplánica: estudio etnobotánico en los Andes de Iquique, Primera Región, Chile. Chungara Revista de Antropología Chilena 31, 81–186.

Villagrán, C., Romo, M., Castro, V., 2003. Etnobotánica del sur de los Andes de la Primera Región de Chile: un enlace entre las culturas Altiplánicas y las de Quebradas Altas del Loa Superior. Chungara Revista de Antropología Chilena 35, 73–124.

Vuille, M., 1999. Atmospheric circulation over the Bolivian Altiplano during dry and wet periods and extreme phases of the Southern Oscillation. International Journal of Climatology 19, 1579–1600.

Vuille, M., Keimig, F., 2004. Interannual variability of summertime convective cloudiness and precipitation in the central Andes derived from ISCCP-B3 data. Journal of Climate 17, 3334–3348.

Vuille, M., Bradley, R.S., Keimig, F., 2000. Interannual climate variability in the Central Andes and its relation to tropical Pacific and Atlantic forcing. Journal of Geophysical Research 105, 12447–12460.

Vuille, M., Bradley, R.S., Healy, R., Werner, M., Hardy, D.R., Thompson, L.G., Keimig, F., 2003a. Modeling $d^{18}O$ in precipitation over the tropical Americas: 2. simulation of the stable isotope signal in Andean ice cores. Journal of Geophysical Research 1008, 4175.

Vuille, M., Bradley, R.S., Werner, M., Healy, R., Keimig, F., 2003b. Modeling $d^{18}O$ in precipitation over the tropical Americas: 1. interannual variability and climatic controls. Journal of Geophysical Research 108, 4174.

Williams, A., Santoro, C.M., Smith, M.A., Latorre, C., 2008. The impact of ENSO in the Atacama Desert and Australian arid zone: exploratory time-series analysis of archaeological records. Chungara Revista de Antropología Chilena 40, 245–259.

Zech, R., Kull, C., Kubik, P.W., Veit, H., 2007. LGM and Late Glacial glacier advances in the Cordillera Real and Cochabamba (Bolivia) deduced from 10Be surface exposure dating. Climate of the Past 3, 623–635.

Zech, R., May, J.-H., Kull, C., Ilgner, J., Kubik, P.W., Veit, H., 2008. Timing of the late Quaternary glaciation in the Andes from 15 to 40°S. Journal of Quaternary Science 23, 635–647.

Zhou, J., Lau, K.-M., 1998. Does a monsoon climate exist over South America? Journal of Climate 11, 1020–1040.